Palaeogeography, Palaeoclimatology, Palaeoecology 684 (2026) 113505

Contents lists available at ScienceDirect

Palaeogeography, Palaeoclimatology, Palaeoecology

journal homepage: www.elsevier.com/locate/palaeo

Sedimentary facies and invertebrate faunal exchange confirm humid conditions in the tropical eastern Atlantic during interglacial Marine Isotopic Stage (MIS) 11c

Carlos S. Melo [a,b,c,d], José Madeira [a,b,c,d], Ricardo S. Ramalho [g,a,c,h], Ana C. Rebelo [f,b,d,e], Michael W. Rasser [f], Esther Martín-González [i], Alfred Uchman [j], Carlos Marques da Silva [a,c], Emílio Rolán [k], Luís Silva [b,l,m], Joseph A. Stewart [n], Laura F. Robinson [n,o], Deirdre D. Ryan [p], Alessio Rovere [p], Antje Voelker [q,r], Patrícia Madeira [b,d,m], Mário Cachão [a,c], Sérgio P. Ávila [b,d,l,m,*]

[a] Universidade de Lisboa, Faculdade de Ciências, Departamento de Geologia, 1749-016 Lisboa, Portugal
[b] CIBIO-Açores – Centro de Investigação em Biodiversidade e Recursos Genéticos, InBIO Laboratório Associado, Pólo dos Açores, Universidade dos Açores, Rua da Mãe de Deus, 9500-321 Ponta Delgada, Açores, Portugal
[c] Universidade de Lisboa, Faculdade de Ciências, Instituto Dom Luiz, 1749-016 Lisboa, Portugal
[d] MPB – Marine Palaeontology and Biogeography Lab, Faculdade de Ciências e Tecnologia, Universidade dos Açores, Rua da Mãe de Deus, 9500-321 Ponta Delgada, Açores, Portugal
[e] Divisão de Geologia Marinha, Instituto Hidrográfico, Rua das Trinas, 49, 1249-093 Lisboa, Portugal
[f] SMNS - Staatliches Museum für Naturkunde Stuttgart, Rosenstein 1, 70191 Stuttgart, Germany
[g] School of Earth and Environmental Sciences, Cardiff University, Park Place, Cardiff CF10 3AT, UK
[h] Lamont-Doherty Earth Observatory, Columbia University, Comer Geochemistry Building, PO Box 1000, Palisades, NY 10964-8000, USA
[i] Museo de Ciencias Naturales de Tenerife, C/ Fuente Morales, s/n, 38003 Santa Cruz de Tenerife, Spain
[j] Faculty of Geography and Geology, Institute of Geological Sciences, Jagiellonian University, Gronostajowa 3a, 30-387 Kraków, Poland
[k] Museo de Historia Natural, Campus Universitario Sur, 15782 Santiago de Compostela, Spain
[l] Departamento de Biologia, Faculdade de Ciências e Tecnologia, Universidade dos Açores, Rua da Mãe de Deus, 9500-321 Ponta Delgada, Açores, Portugal
[m] BIOPOLIS/CIBIO - Biodiversity and Genetic Resources Research Center, Universidade do Porto, Campus de Vairão. Rua do Crasto, n° 765, 4485-684 Vairão, Portugal
[n] School of Earth Sciences, University of Bristol, Wills Memorial Building, Queen's Road, Bristol BS8 1RJ, UK
[o] Department of Environment and Geography, University of York, York, UK
[p] MARUM – Center for Marine Environmental Sciences, University of Bremen, Bibliothekstraße 1, 28359 Bremen, Germany
[q] IPMA – Instituto Português do Mar e da Atmosfera, Avenida Alfredo Magalhães Ramalho, 6, 1495-165 Algés, Portugal
[r] CCMAR – Centro de Ciências do Mar, Universidade do Algarve, Campus de Gambelas Edifício 7, 8005-139 Faro, Portugal

ARTICLE INFO

Editor: Howard Falcon-Lang

Keywords:
Pleistocene
MIS 11c
Palaeoenvironment
Sheltered bay
Senilia senilis
Volcanic oceanic islands

ABSTRACT

The geological study of Marine Isotopic Stage (MIS) 11c (424–397 ka) is key to reconstructing the climatic and oceanographic conditions during one of the longest and the warmest interglacial in the last 1 million years. Moreover, interglacial MIS 11c is considered as an important analogue for our near future in times of climate change, under anthropogenic emissions scenarios, due to its similar orbital forcing configuration. Here we present the results of a comprehensive analysis of one of the most extensive Quaternary fossiliferous sedimentary successions in the Cabo Verde archipelago in the tropical northeastern Atlantic. The Nossa Senhora da Luz Bay (Santiago Island) is one of the few MIS 11 fossiliferous sites known in Macaronesia. The sedimentary succession records a set of transitions between fluvial and marine environments, and emersion and immersion events within a confined, highly protected bay environment. A thick layer of fine-branched rhodoliths in its upper part suggests ecological conditions that no longer exist in Cabo Verde. The presence of specimens of the intertidal clam *Senilia senilis* in life position ~12 m above present-day mean sea level leads us to reinterpret the relative sea-level changes at Santiago Island and show that the uplift trend since MIS 11c is an order of magnitude lower (0.01 mm/yr) than previously calculated (0.10 to 0.14 mm/yr). The fossil assemblage includes representatives of five

* Corresponding author at: CIBIO-Açores – Centro de Investigação em Biodiversidade e Recursos Genéticos, InBIO Laboratório Associado, Pólo dos Açores, Universidade dos Açores, Rua da Mãe de Deus, 9500-321 Ponta Delgada, Açores, Portugal.
E-mail address: avila@uac.pt (S.P. Ávila).

https://doi.org/10.1016/j.palaeo.2025.113505
Received 15 July 2025; Received in revised form 12 December 2025; Accepted 14 December 2025
Available online 16 December 2025

phyla, with molluscs being the most diverse and abundant. Despite the abundance of some bivalves (*Saccostrea cucullata*, *S. senilis*, and *Aequipecten opercularis*), and gastropods (*Thetystrombus latus* and *Thais nodosa*), and some horizons showing the crustacean burrows *Thalassinoides suevicus*, the general biodiversity is low. The presence of *S. cucullata* and *S. senilis*, both absent from present-day Cabo Verde archipelago, indicates a tropical, more humid climate in this region, during MIS 11c.

1. Introduction

Sea-level changes have a considerable impact on the marine biota of volcanic oceanic islands (Ávila et al., 2019). Past glacial-interglacial cycles led to significant glacio-eustatic oscillations, dramatically impacting habitable littoral area, as well as to important changes in mean sea-surface temperatures (SSTs). Both phenomena are connected to profound ecological changes in local ecosystems and in overall species distribution, drastically transforming the structure of insular bio-communities (Budd et al., 1996; Ávila et al., 2019). These changes are more pronounced when comparing the maxima of interglacial (Stirling et al., 1998; Meco et al., 2002; Ávila et al., 2009a; Zazo et al., 2010; Garilli, 2011; Montesinos et al., 2014; Muhs et al., 2014; Ávila et al., 2015b; Martín-González et al., 2016, 2019; Ávila et al., 2019) and glacial episodes (Lea et al., 2000; Amano, 2004; Monegatti and Raffi, 2007, 2010; Ávila et al., 2018a; Yokoyama et al., 2018), when extremes of mean sea levels (msl) and SSTs are reached. Similarly, it is during stillstands that marine abrasion surfaces are formed, often acting as loci for the deposition of coastal sediments (Trenhaile, 1989, 2001, 2002; Ramalho et al., 2013; Ricchi et al., 2018). Marine terrace sedimentary successions formed during interglacials, especially during highstand maxima, are more likely to be preserved (Rovere et al., 2016). Their preservation, however, largely depends on their shielding from subsequent marine erosion by younger highstands, and from ensuing sea level heights not reaching them (Ricchi et al., 2018; Bulian et al., 2025). Although uncommon, interglacial marine terraces constitute prime localities to look for biological and environmental records, providing unique insights into periods which had a different climate from today.

Two significant interglacials of the past 800 ka are the Marine Isotopic Stages (MIS) 11c (424–397 ka) and 5e (129–115 ka) (Rohling et al., 2010; Govin et al., 2015; Past Interglacials Working Group of PAGES, 2016). During these periods, msl was 6 to 13 m (MIS 11c) and 6 to 9 m (MIS 5e) higher than present (Raymo and Mitrovica, 2012; Dutton and Lambeck, 2012; Hansen et al., 2015; Spratt and Lisiecki, 2016; Hearty and Tormey, 2017), with temperatures up to 3 °C higher than modern (Clark and Huybers, 2009; Kleinen et al., 2014; Hoffman et al., 2017). However, the MIS 11c is the longest interglacial of this period, lasting for around 30 ky (McManus et al., 2003; Tzedakis et al., 2012) and, despite being a good analogue for the present-day interglacial (Loutre and Berger, 2003), the MIS 11c extended over two insolation peaks, with precession and obliquity in almost opposing phase, unlike our current interglacial (Tzedakis et al., 2022). These environmental

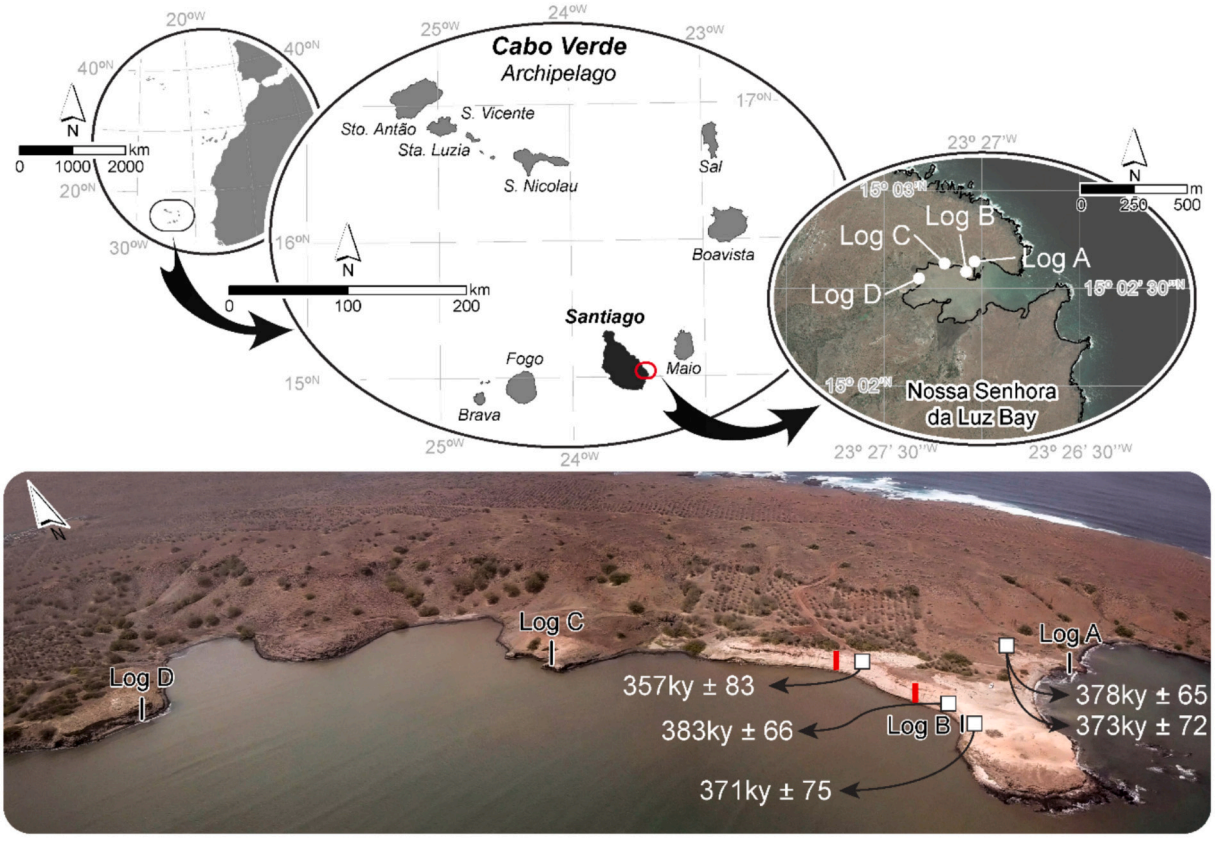

Fig. 1. Geographical framework of Santiago Island within the tropical East Atlantic. Photo insert of Nossa Senhora da Luz Bay. The black vertical lines on the photo mark the locations of Logs A to D. White squares indicate coral dating sites. Red rectangles indicate the sectors where calcareous nannofossil were collected (at the base, middle and top of the stratigraphic succession). Present-day coastline obtained from Portuguese Instituto Hidrográfico (2019) data. Orthophotomap from Unidade de Coordenação do Cadastro Predial (UCCP) from Ministério do Ambiente, Habitação e Ordenamento do Território, Cabo Verde. (For interpretation of the references to colour in this figure legend, the reader is referred to the web version of this article.)

Table 1
Sediment analysis and classification according to Folk and Ward (1957) and Flemming (2000).

ID	Mean diameter (ϕ)	Dispersion (1σ)	Asymmetry (SKI)	Kurtosis (KS)	% of coarse sediments	% of fine sediments	Size (after Wentworth, 1922)	Based on Folk and Ward (1957)			Textural class (Flemming, 2000)
								Calibration	Asymmetry	Kurtosis	
1	1.23	1.95	−0.18	0.73	16.67	83.33	Medium sand	Poorly calibrated	Negative asymmetry	Platykurtic	Slightly sandy mud
2	0.24	1.93	−0.06	0.76	59.36	40.64	Coarse sand	Poorly calibrated	Almost symmetric	Platykurtic	Muddy sand
3	0.23	1.94	0.16	0.72	42.98	57.02	Coarse sand	Poorly calibrated	Positive asymmetry	Platykurtic	Sandy mud
4	0.29	2.02	0.11	0.69	22.50	77.50	Coarse sand	Poorly calibrated	Positive asymmetry	Platykurtic	Slightly sandy mud
5	1.32	2.03	−0.24	0.63	29.20	70.80	Medium sand	Poorly calibrated	Negative asymmetry	Platykurtic	Sandy mud
6 *	2.28	0.59	−0.22	1.32	5.45	94.55	Fine sand	Moderately calibrated	Negative asymmetry	Leptokurtic	Slightly sandy mud
7 *	1.78	1.53	−0.38	0.89	94.84	5.16	Medium sand	Poorly calibrated	Negative asymmetry	Platykurtic	Slightly muddy sand

* Sediment samples collected from the present-day tidal flat of the Nossa Senhora da Luz Bay.

conditions impacted marine insular biological communities worldwide, such as those in the archipelagos of the Macaronesian region (Fig. 1): the Azores (Ávila et al., 2008, 2009a, b, 2015a, b); Madeira (Gerber et al., 1989); Selvagens (García-Talavera and Sánchez-Pinto, 2001); Canary Islands (Zazo et al., 2002; Meco et al., 2002; Zazo et al., 2003a, 2003b; Montesinos et al., 2014; Muhs et al., 2014; Martín-González et al., 2016, 2019); and Cabo Verde (Zazo et al., 2007, 2010). As a result, local disappearance (extirpation) – and in some cases, species extinction – occurred. However, speciation also took place, resulting in noticeable changes in the biodiversity of insular marine ecosystems (Hachich et al., 2015; Ávila et al., 2016a, 2016b, 2018b, 2019; Hachich et al., 2019; Melo et al., 2022a, 2022b; see Table 1.)

The identification of the highest position of past relative sea levels in insular volcanic edifices is key to understand the evolutionary history of oceanic islands, namely, to accurately establish their uplift, static or subsidence trends. Stratigraphic palaeo-relative-sea-level markers, as defined by Ramalho (2011) are visible on the island shores, often as wave-cut notches. The shore angle of palaeoshorelines (i.e., the angle of the inner edge of marine terraces), together with wave-cut notches, are commonly used to deduce, with great accuracy and resolution, the relative-sea-level position coeval of that shoreline (Rovere et al., 2016), which in turn allows to estimate vertical land movement rates. Well-preserved palaeo-relative-sea-level markers in the geological record of oceanic islands are common for the MIS 5e interglacial. However, they are quite rare for the older MIS 11c interglacial (Hearty et al., 1999).

Likewise, well-preserved Quaternary interglacial fossiliferous marine sequences are also rare in active volcanic ocean islands, because they are usually subjected to pronounced subsidence (Ramalho et al., 2013). Such occurrences, however, are key to understanding past environments and palaeobiodiversity, allowing us to better predict the effects that future climate change will have on mid-ocean living communities (Doney et al., 2012).

Numerous studies have investigated the present-day marine Macaronesian fauna and flora (see Freitas et al., 2019, and references therein). However, only some of these studies focused on the Macaronesian palaeobiodiversity (Supplementary data 1 for list of works), with the northern archipelagos receiving more attention. By contrast, for the Cabo Verde archipelago, studies on marine palaeobiodiversity are scarce and mainly focused on macrofossils (Lecointre and Serralheiro, 1966; Serralheiro, 1967, 1976; Mitchell-Thomé, 1976; García-Talavera, 1999; Johnson et al., 2012; Baarli et al., 2013, 2017) and trace fossils (Baarli et al., 2013; Mayoral et al., 2013; Santos et al., 2015; Mayoral et al., 2018). This knowledge gap severely hampers understanding the marine palaeobiogeography of the region during Quaternary interglacial periods.

Santiago is the largest Cabo Verdean island (Fig. 1), with a complex geological history dating back to the Late Miocene to Early Pliocene (Ramalho et al., 2010a, 2010b, 2010c; Ramalho, 2011). The island exhibits well exposed Miocene-Pliocene marine fossiliferous sedimentary successions (Serralheiro, 1976; Ramalho et al., 2010a, 2010b, 2010c; Ramalho, 2011), Pleistocene marine fossiliferous deposits (Johnson et al., 2012; Baarli et al., 2013; Mayoral et al., 2018), and tsunamigenic deposits (Paris et al., 2011; Ramalho et al., 2015b; Paris et al., 2018; Madeira et al., 2020; Costa et al., 2021). However, mentions of Quaternary interglacial marine sedimentary successions were made only by Serralheiro (1967, 1976), Madeira et al. (2010), and Ramalho (2011). Atlantic volcanic island MIS 11c sedimentary successions are only reported from Gran Canaria and Lanzarote (Canary Islands; Zazo et al., 2002; Montesinos et al., 2014; Muhs et al., 2014; Clauzel et al., 2020), and possibly from Santo Antão (Cabo Verde; Ramalho, 2011).

Herein, we report and discuss a peculiar, in the context of volcanic oceanic islands, very sheltered, low energy, and remarkably well-preserved MIS 11 marine fossiliferous sedimentary succession exposed within the Nossa Senhora da Luz Bay on Santiago Island, Cabo Verde. We examine its sedimentological and morphological features, as well as its biodiversity. The stratigraphic age control in this study is provided by

new Uranium/Thorium (U/Th) dates performed on fossil corals, and by nannofossil biostratigraphy. Finally, we use our findings to reconstruct the palaeoecological and environmental conditions through the lengthy MIS 11 interglacial and to frame the coeval Cabo Verde marine fauna in a tropical East Atlantic palaeoclimatic and palaeobiogeographical context.

2. The Cabo Verde archipelago: A geographic, geological, and geomorphological framework

Located 600 km off the western coast of Africa, the Cabo Verde archipelago consists of 10 volcanic islands and a few islets, with the oldest ages of subaerial volcanic rocks ranging from 15.8 Ma in Sal to <3 Ma in Fogo Island (Ramalho, 2011; Fig. 1). The origin of the archipelago is attributed to the Cabo Verde hotspot, with volcanic activity ranging from the Oligocene (Ramalho, 2011) to the present (Fogo 2014–15 volcanic eruption; Mata et al., 2017). Santiago (15°N, 23.5°W) is the largest island and one of the four islands that make up the leeward group of the archipelago. This island presents several exposures of fossiliferous sedimentary successions, ranging in age from Miocene to Quaternary (e.g., Serralheiro, 1967, 1976).

The earliest accounts of the geology of Santiago were produced by

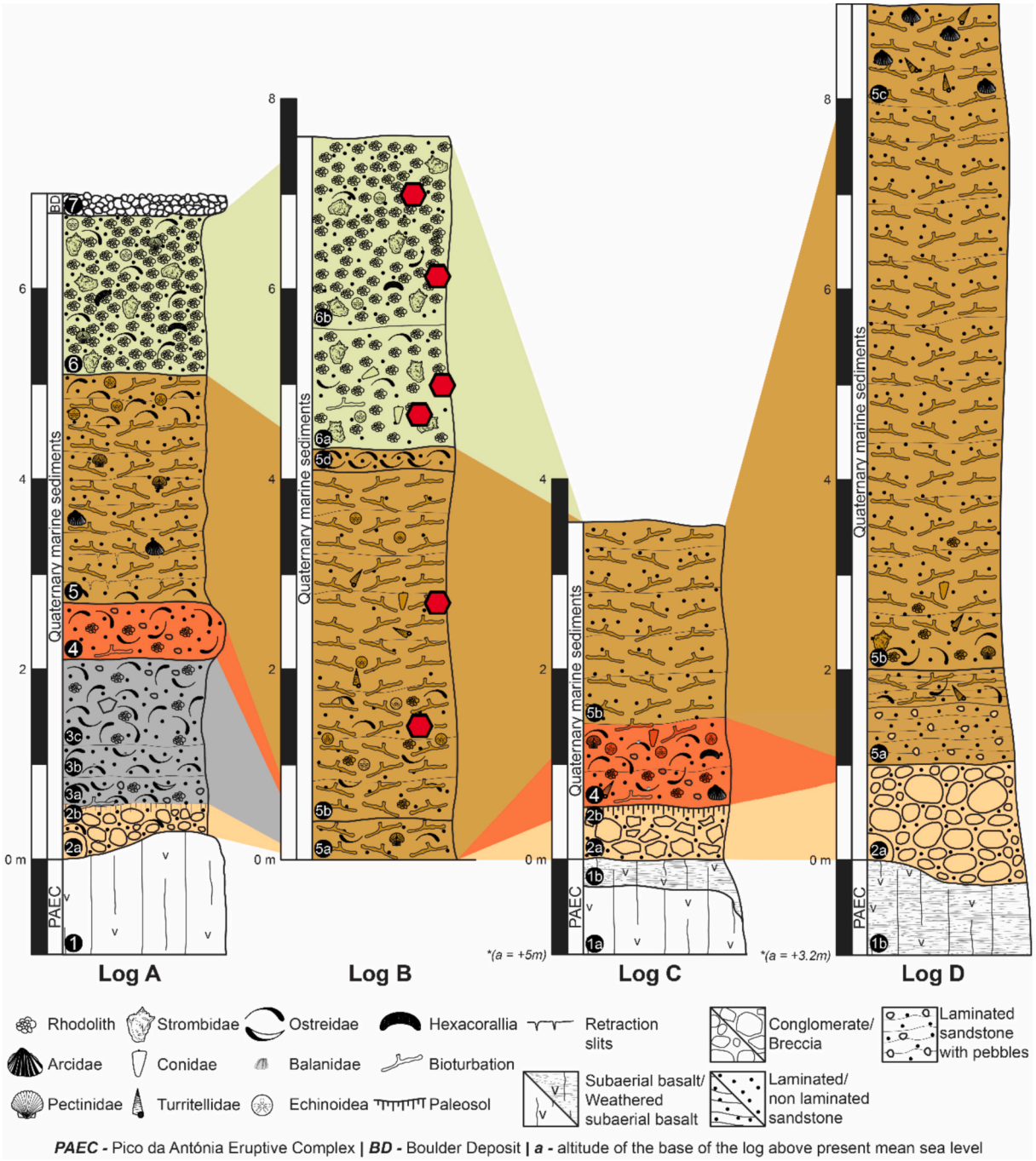

Fig. 2. Stratigraphic logs from Nossa Senhora da Luz Bay fossiliferous sections, with correlation between them. Red hexagons indicate the position where samples for nannofossil analysis were collected. PAEC – Pico da Antónia Eruptive Complex; BD – Boulder Deposit. Geological units are in accordance with the geological map of Santiago Island (Serralheiro, 1976). The sedimentological analysis was performed on five samples that were collected from layers 2a, 3a, 3b, 3c and 4, across log A. (For interpretation of the references to colour in this figure legend, the reader is referred to the web version of this article.)

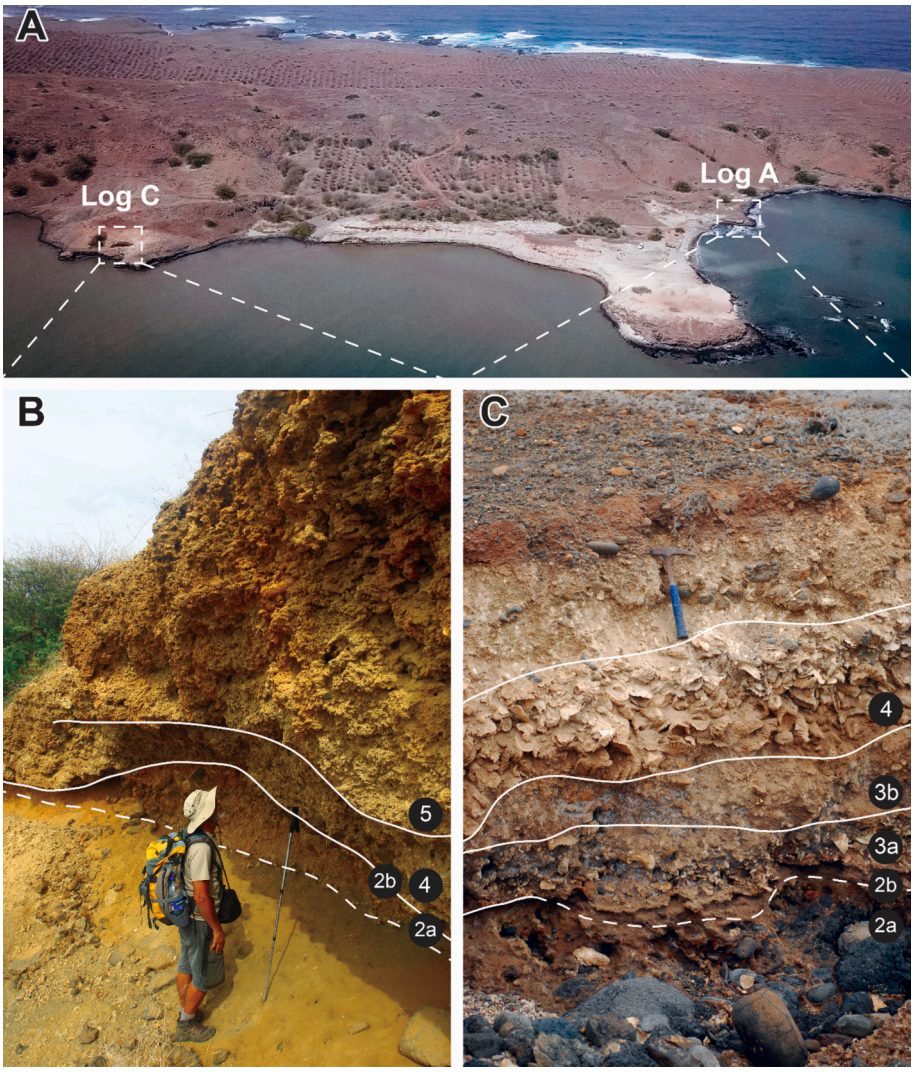

Fig. 3. General and detailed views of the MIS 11c deposits at Nossa Senhora da Luz Bay. A: General view of the Eastern part of the study area. The dashed squares mark the location of Logs C (Fig. 3B) and A (Fig. 3C); B: General view of the stratigraphic succession in Log C location; C: General view of the stratigraphic succession in Log A location. Dashed white lines represent the transition between sub-layers; solid white lines represent the location of the transition between layers. The numbers of the layers are the same as in Fig. 2.

Darwin (1839, 1844), and later by Bebiano (1932). A summary of Santiago's volcanostratigraphic history is presented in Supplementary data 2. The MIS 11 studied sequence is part of a 'Quaternary unit' composed of sediments resulting from marine erosion (Serralheiro, 1967, 1976). The MIS 11 terraces are associated with marine abrasion surfaces carved on the Pico da Antónia Eruptive Complex basalts, also showing signs of subaerial erosion (Serralheiro, 1967, 1976).

Nossa Senhora da Luz Bay (15.044°N, 23.452°W) is a peculiar geomorphological feature in the context of the Macaronesian islands. This type of sheltered bay with a narrow inlet is uncommon in eastern Atlantic islands. Similar bays are more common in western Atlantic Ocean archipelagos (Supplementary data 3). However, the occurrence of Quaternary interglacial marine fossiliferous sedimentary successions in such sheltered bays is only known to us from Santa Martha Bay (Curaçao Island; MIS 5e; del Valle, 2012), with Nossa Senhora da Luz Bay being just the second reported for the Atlantic Ocean.

3. Materials and methods

3.1. Stratigraphy and fossil content

To fully represent the facies variation, four stratigraphic logs were compiled at different locations across the bay. The outcrop is located on the north bank of the bay, following an East-West direction (Fig. 1, logs A to D). Bulk samples of 1 kg each were collected along the sedimentary succession, later sorted, and its fossil content analysed in the laboratory using a Leica Zoom 2000 stereomicroscope. All material collected is stored at the fossil reference collection of the Department of Biology of the University of the Azores, (DBUA-F 1256, 1301, 1310, 1314, 1318, 1319, 1320; 1331; 1403, 1404, 1405, 1406, 1407, 1408, 1423, 1424 and 1425). All Mollusca from these bulk samples were sorted in the laboratory, counted, and identified; search sampling of fossil specimens was also performed along the sedimentary succession and later sorted and identified in the laboratory (Supplementary Fig. S1).

A quantitative survey of modern taxa was done on a 90-m transect laid down along the bay-shore in the vicinity of Log B. The remains of Holocene invertebrates were collected, sorted, and identified using the same methodology as for the fossil samples. The present-day specimens are stored at the reference collection of the Department of Biology of the University of the Azores, (DBUA 1395, 1396, and 1398). Species nomenclature and authority are in accordance with the World Register of Marine Species (WoRMS Editorial Board, 2023).

All molluscan data from the bulk and qualitative search samples is shown in Supplementary Table S1. Notes were taken from the

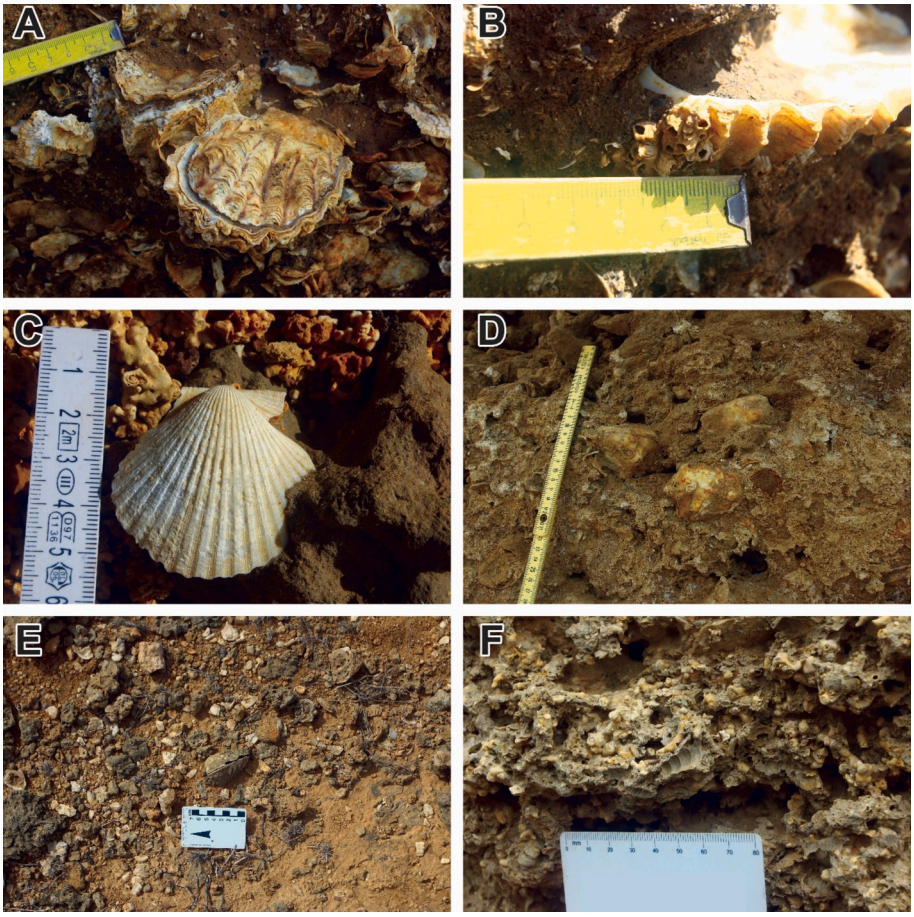

Fig. 4. Specimens of the fossil assemblage. A: In situ *Saccostrea cucullata* (Log A); B: Balanidae on *S. cucullata* (Log A); C: Right valve of *Aequipecten opercularis* (Log B); D: Several *Thetystrombus latus* (Log C); E: *Senilia senilis* in living position (plan view; top of Log D); F: External mould of *Turritella bicingulata* (Log C).

PaleoBiology Database (https://paleobiodb.org/), regarding species biological and ecological traits, namely data on larval development, mineralogy of the shell, life habit (infaunal or epifaunal), type of mobility/locomotion, trophic group, substrate type, the average SST, expressed as a whole environmental envelope (tropical, subtropical), and the type of habitat.

3.2. Biostatistics

Analyses were performed using R version 4.2.0 (R Core Team, 2022). Severgal R packages were used, namely: vegan (Oksanen et al., 2017), ade4 (Dray and Dufour, 2007), cluster (Maechler et al., 2018), gclus (Hurley, 2012), and recluster (Dapporto et al., 2015). Dendrograms depicting the relationships between areas were constructed, using dissimilarity indices and cluster analysis. Several classical distance metrics for presence/absence data were applied, namely Jaccard, Sørensen, Ochiai and Simpson dissimilarities (Jaccard, 1901; Sørensen, 1948; Ochiai, 1957; Simpson, 1960). Furthermore, for each dissimilarity coefficient, several agglomeration methods were tested (Legendre and Legendre, 1998), namely complete linkage, centroid distance, unweighted pair group method with arithmetic mean (UPGMA), and Ward's minimum variance clustering (Ward, 1963). To determine the best combination of dissimilarity measure and agglomeration method, the cophenetic correlation value between the region's distance matrix and the dendrogram representation was calculated (Sokal and Rohlf, 1962). The guidelines defined in Borcard et al. (2011), and the hierarchical clustering approach reported by Pavão et al. (2019) were followed. For the dendrogram, the putative number of groups formed by the target regions was estimated using both the Rousseeuw quality index, that determines the optimal number of clusters according to silhouette widths (Rousseeuw, 1987) and the Mantel statistic, that determines the optimal number of clusters according to Mantel statistic (Pearson) (Legendre and Legendre, 1998). For dendrogram implementation the guidelines of Borcard et al. (2011) and Pavão et al. (2019) were followed. This was further supported by a bootstrap validation procedure, implemented using the Recluster package, which provides robust techniques to analyse patterns of similarity in species composition (Kreft and Jetz, 2010; Dapporto et al., 2013, 2014, 2015). Each dendrogram was targeted by a resampling procedure with 100 trees per iteration and a total of 1000 iterations. All the dissimilarity coefficients were retested using this approach, to ensure consistency in the number of groups formed by the target regions, for each taxonomic group.

3.3. Sediment analysis

Seven sediment samples were collected: five from the studied fossiliferous sequence (one from each layer 2a, 3a, 3b, 3c and 4, across log A; samples 1–5; cf. Fig. 2) and two from present-day tidal flat sediments (samples 6 and 7). Samples 6 and 7 were collected near the location of Log B at, respectively, 1.5 and 3 m from the margin at low tide. These samples were analysed at the Sedimentology Laboratory of the Geology Department of the University of Lisbon. Graphic mean, median, standard deviation, skewness, and kurtosis were obtained using Folk and Ward (1957) methodology. Due to the richness in carbonate bioclasts, some samples were decalcified.

Six samples for calcareous nannofossil samples were collected from the most favourable layers, with fewer coarse bioclasts and a rich fine carbonate matrix (see Figs. 1 and 2). In the laboratory, approximately

one-third of a test tube of sediment was vigorously mixed with tap water and left to settle for 24 h. A small portion of the uppermost, finest fraction was then extracted using a Pasteur pipette and directly smeared onto a cover glass. The resulting ripple-textured smear was dried and permanently mounted onto a slide using synthetic resin (Entellan). For each sample, an entire 30 mm length of the smear slide was examined for nannoliths using a petrographic microscope (Leica DM2700P with Leica Flexcam C1) at 1250× magnification.

3.4. Laser-ablation U/Th disequilibrium geochronology

In total, six coral fossil specimens (*Siderastrea radians*) were collected and dated using U/Th disequilibrium geochronology from the middle and top of the sequence (corals are absent at the base of the sequence) corresponding to samples ST84–1, ST84–3, ST85–1, and STG34–2 from the middle of the sequence, and ST86–1 and STG-34-4, from the top of the sequence (ST = STG: Santiago).

The sampled fossils of corals had no visible signs of recrystallization and were processed, cut, and polished for analysis at the University of Bristol, following established protocols outlined in Spooner et al. (2016). For dating, the half-lives method reported in Cheng et al. (2000) was used. The samples were laser-ablated using a Photon Machines Analyte G2 193 nm laser. ^{230}Th and ^{238}U isotopes were measured using a Neptune Multi-Collector Inductivity Coupled Plasma Mass Spectrometer (MC-ICP-MS) on a central ion counter and a Faraday cup respectively. Ages were calculated using ^{230}Th/^{238}U ratios corrected for background (laser cell gas blank), assuming that there has been no open-system behaviour and that initial ^{230}Th was negligible. Ages were calculated by Newton-Raphson iteration and scaled to the in-house inorganic aragonite standard VS001. This technique is routinely applied to carbonate samples <350 ka in age and age uncertainty greatly inflates as samples approach ages of 400 ka and secular equilibrium (Spooner et al., 2016). This method does however allow carbonate samples from younger interglacial intervals (i.e. MIS 9e or younger) to be distinguished from previous interglacials like MIS 11c (400 ka).

3.5. Topographic survey

The present-day maximum altitude of the studied fossiliferous sedimentary succession was measured using a single-band differential GPS, Emlid Reach RS+. Delimitation of the outcrop was made both in the field, and by using high-resolution aerial photography acquired by unmanned aerial vehicle (UAV) DJI Mavic Pro, with native camera attached. An UAV orthomosaic map was compiled using "DroneDeploy" photogrammetry tools. A Digital Elevation Model (DEM, 2010) from Santiago Island was computed using ArcGIS 10.2.2, to which the delimitation of the Hydrographic Basin that drains into Nossa Senhora da Luz Bay was added. An additional airborne orthophotomap (50 cm of spatial resolution) and altimetric information from Santiago Island were also used, provided by Unidade de Coordenação do Cadastro Predial (UCCP) from Ministério do Ambiente, Habitação e Ordenamento do Território, Cabo Verde Republic.

4. Results

4.1. Stratigraphic logs

Four sections (Logs A, B, C, and D) were measured along the northern coast of Nossa Senhora da Luz Bay (Fig. 1). Except for Log B, where the base of the sequence is not exposed, all the sedimentary sequences measured start on an erosion surface carved on subaerial basalts (i.e., a shore platform).

4.1.1. Log A

The stratigraphic succession recorded in Log A lies on subaerial basalts from the Pico da Antónia Eruptive Complex (sub-layer 1a, Figs. 2, 3A, C). It starts as a 20 to 55 cm-thick coarse gravel deposit composed of both rounded and angular clasts on a silty-clay matrix, more abundant at the top (sub-layer 2a, Logs A, C and D, Fig. 2). In situ fossil specimens of the bivalve *Saccostrea cucullata* (Born, 1778; Fig. 4A and B) were found attached to the bedrock and boulders (sub-layer 2a, Fig. 2). A paleosol (sub-layer 2b) is developed on top of sub-layer 2a, separating it from sub-layer 3a (Log A, Figs. 2, 3C).

The deposit represented in layer 3 is present only in Log A and can be divided in three sub-layers. Sub-layer 3a is a silty sand containing occasional pebbles. This layer is rich in specimens of *S. cucullata*, varying in size from 5 to 15 cm, some of which articulated (Fig. 3C), scarce rhodoliths and bioturbation structures. The burrows, *Thalassinoides suevicus* (Rieth, 1932), generally assigned to the burrowing activity of crustaceans, have an average diameter of 5 cm. Sub-layer 3b is a silty clay with thicknesses, from 0 to 35 cm. In this layer *S. cucullata* is less abundant and valves are often incrusted with balanids; specimens with articulated valves were not observed (Fig. 4B). Sub-layer 3c corresponds to a 70 to 90 cm-thick coquina composed almost exclusively of disarticulated valves of *S. cucullata*. Sporadic poorly preserved rhodoliths are also present at the top. The silty-clay matrix includes occasional rounded (up to 5 cm in diameter) and rare angular basalt clasts (up to 15 cm in diameter). In all sub-layers of layer 3, valves of *S. cucullata* are present, both pristine and bored with clionaid sponges (trace fossil *Entobia* isp.).

Layer 4 is present in Logs A and C (Fig. 2) and corresponds to a 60 cm-thick, bioturbated clay bed, containing scattered rhodoliths, fragments of bivalve shells and internal and external moulds of gastropods (e.g., *Turritella bicingulata* Lamarck, 1822).

Layer 5 (Fig. 2) is a stratigraphic succession of thin silt levels that ranges from 2.0 m (Log C) to 8.0 m-thick (Log D), and is divided into four sub-layers. The lowermost level presents desiccation cracks indicating temporary emersion. Disarticulated valves of *S. cucullata* are present in the lowermost sub-layer 5a, absent in the intermediate ones, and become abundant in the upper sub-layer 5d (cf. Log B, Fig. 2). Other bivalve species, such as *Aequipecten opercularis* (Linnaeus, 1758) (Fig. 4C) and *Senilia senilis* (Linnaeus, 1758) (Fig. 4E) are present but less frequent, together with echinoid spines (cf. *Eucidaris* sp.), while gastropods are represented by poorly preserved moulds of *T. bicingulata* (Fig. 4F). The whole stratigraphic succession is heavily bioturbated with *Thalassinoides suevicus*, forming large, slightly oblique, simple, straight, subcylindrical burrows, probably produced by crabs.

Layer 6 corresponds to a 1.7 (Log A) to 3.3 m-thick rhodolith deposit (Log B, Fig. 2). This layer is the one that presents higher biodiversity, with large, disarticulated specimens of *S. cucullata*, *Thetystrombus latus* (Gmelin, 1791) (Fig. 4D), *A. opercularis*, spines of cidaroid and *Echinometra* echinoids, and corals, but also smaller specimens of the bivalve *Arcopsis afra* (Gmelin, 1791) and the gastropod *Volvarina* sp. Some shells show serpulid incrustations. The stratigraphic succession in Log A is topped by layer 7, a present-day boulder colluvium (Fig. 2) resulting from mechanical erosion of nearby basaltic outcrops.

4.1.2. Log B

In Log B, unlike Logs A, C, and D (Fig. 2), the basement is not exposed above present-day mean sea level. The subaerially exposed stratigraphic succession begins with layer 5 of the overall sequence. The lowermost bed is a 40 cm-thick highly bioturbated clay (sub-layer 5a) containing dispersed rhodoliths and specimens of *A. opercularis*. It is covered by a 3.7 m-thick level of heavily bioturbated clayey-silty sands (sub-layer 5b), presenting horizontal bedding. It contains scattered rhodoliths, rare specimens of *S. cucullata*, *A. opercularis*, *Conus* spp., moulds of *T. bicingulata*, and echinoid spines. Sub-layer 5d is a 20 cm-thick coquina, composed of an accumulation of *S. cucullata* shells, occasionally articulated.

Layer 6 is composed of two sub-layers: sub-layer 6a is a 120 cm-thick silty-clayey sandstone slightly bioturbated, containing rhodoliths, *Conus* spp., *S. cucullata* and *T. latus*. Upwards this layer changes into a

Table 2
Comparison between fossil molluscs from the MIS 11c sediments and recent molluscs from the present-day tidal flat. * Reported by Serralheiro (1976); ** reported by Serralheiro (1976) but not found in our surveys. Pr/Ab: Presence/Absence: 1 - present; 1^{+} – probable presence. Species occurring in both MIS 11c sediments and in the present tidal shore are highlighted.

Taxonomic composition	Quantitative Samples									
	MIS 11c							Recent		
Species / Taxa	Pr/Ab	Log A	Log B	Log C	Log D	TOTAL	%	Pr/Ab	TOTAL	%
Aequipecten opercularis (Linnaeus, 1758) *	1	16	37		4	**57**	***18.15***			
Alvania cf. *peli* Moolenbeek & Rolán, 1988	1		1			**1**	***0.32***			
Arca noae Linnaeus, 1758								1	**6**	***1.57***
Arca tetragona Poli, 1795 **	1	-	-	-	-	**?**				
Arcopsis afra Gmelin, 1791)	1		6			**6**	***1.91***	1	**8**	***2.10***
Bulla cf. *striata* Bruguière, 1792								1	**7**	***1.84***
Bursa scrobilator (Linnaeus, 1758)	1		2			**2**	***0.64***	1	**1**	***0.26***
Caecum sp.	1		1			**1**	***0.32***			
Cerithium cf. *atratum* (Born, 1778)	1				1	**1**	***0.32***	1	**1**	***0.26***
Chama cf. *gryphoides* Linnaeus, 1758								1	**1**	***0.26***
Columbella adansoni Menke, 1853								1	**1**	***0.26***
Conus sp.	1		3	2	2	**7**	***2.23***	1	**7**	***1.84***
Cymbula safiana (Lamarck, 1819)								1	**1**	***0.26***
Cypraecassis testiculus senegalica (Gmelin, 1791)								1	**3**	***0.79***
Dendropoma sp.	1		6			**6**	***1.91***			
Euthria cf. *helenae* Rolán, Monteiro & Fraussen, 2003	1		1			**1**	***0.32***			
Fissurella sp.	1		1			**1**	***0.32***	1	**16**	***4.20***
Gari fervensis (Gmelin, 1791) **	1	-	-	-	-	**?**				
Gastrana fragilis (Linnaeus, 1758) **	1	-	-	-	-	**?**				
Gemophos viverratus (Kiener, L.C., 1834)								1	**51**	***13.39***
Hexaplex cf. *rosarium* (Röding, 1798)	1		2			**2**	***0.64***	1	**1**	***0.26***
Hipponix cf. *antiquatus* (Linnaeus, 1767)								1	**4**	***1.05***
Hipponix cf. *subrufus* (Lamarck, 1822)	1		1			**1**	***0.32***		**23**	***6.04***
Hyotissa virleti (Deshayes, 1832) **	1	-	-	-	-	**?**				
Isognomon dunkeri (P. Fischer, 1881)								1	**8**	***2.10***
Jujubinus cf. *rubioi* Rolán & Templado, 2001	1		2		1	**3**	***0.96***			
Leporimetis papyracea (Gmelin, 1791) **	1	-	-	-	-	**?**				
Loripes cf. *orbiculatus* Poli, 1795								1	**16**	***4.20***
Luria lurida (Linnaeus, 1758)								1	**12**	***3.15***
Megaxinus sp.								1	**3**	***0.79***
Naria spurca (Linnaeus, 1758)								1	**4**	***1.05***
Nerita senegalensis Gmelin, 1791								1	**102**	***26.77***
Patella sp.**	1	-	-	-	-	**?**				
Thetystrombus latus (Gmelin, 1791) *	1	1	16		2	**19**	***6.05***	1^{+}		
Phorcus cf. *mariae* Templado & Rolán, 2012								1	**5**	***1.31***
Saccostrea cucullata (Born, 1778) *	1	24	69	2	6	**101**	***32.17***			
Schwartziella cf. *puncticulata* Rolán & Luque, 2000	1		1			**1**	***0.32***			
Senilia senilis (Linnaeus, 1758) *	1	2	48	2	10	**62**	***19.75***			
Siphonaria cf. *pectinata* (Linnaeus, 1758)								1	**10**	***2.62***
Spondylus senegalensis Schreibers, 1793	1			1		**1**	***0.32***	1	**1**	***0.26***
Stramonita haemastoma (Linnaeus, 1767)								1	**3**	***0.79***
Tagelus cf. *adansonii* (Bosc, 1801)								1	**8**	***2.10***
Thais nodosa (Linnaeus, 1758) *	1		11			**11**	***3.50***	1	**63**	***16.54***
Thyasira sp.**	1	-	-	-	-	**?**				
Turritella bicingulata Lamarck, 1799*	1	1		3	23	**27**	***8.60***	1	**14**	***3.67***
Venus sp.**	1	-	-	-	-	**?**				
Vermetus sp.	1		3			**3**	***0.96***			
Volvarina sp.								1	**1**	***0.26***
TOTAL	29	44	211	10	49	**314**	***100***	29	**381**	***100***

rhodolith bed (sub-layer 6b), devoid of sediment matrix. Besides the dominant rhodoliths, fragments of *S. cuccullata*, coral fragments, echinoid spines, and well-preserved specimens of *T. latus* are also embedded within the rhodolith bed.

4.1.3. Log C

The sedimentary succession lies on basaltic subaerial lava flows (sub-layer 1a), whose top is intensely weathered (sub-layer 1b; Fig. 3B). A 35 to 55-cm thick fluvial deposit, mainly composed of angular basaltic submarine lava flow clasts (sub-layer 2a), covers the basal lava flows, and presents a well-developed 20 cm-thick paleosol (sub-layer 2b) at the top (Log C, Fig. 2). The base of the marine sedimentary succession stands at approximately 6.5 m above msl and starts with layer 4. This unit is a 1 m-thick fine sand layer with scattered basalt clasts, rich in *S. cuccullata* fossils in the lowermost 60 cm, some in situ, still attached to basaltic boulders and showing encrusting barnacles; the oyster abundance decreases upwards. Specimens of *T. bicingulata*, *A. opercularis*, *S. senilis*, *Conus* spp., rhodoliths, spines of echinoids, serpulids and rare coral fragments are also present. The sandy matrix is bioturbated by unidentified vertical burrows.

Layer 5 is represented by sub-layer 5b and corresponds to a 2 m-thick silty-clayey sandstone highly bioturbated with vertical, oblique, and horizontal *T. suevicus*.

4.1.4. Log D

As in Log C, the marine sedimentary succession lies on a subaerial basaltic basement, having its base ~5.2 m above msl. The basement is composed of strongly weathered subaerial basaltic lava flows (sub-layer 1b). It is overlain by a 1 to 2-m thick fluvial pebble/boulder deposit (sub-layer 2a). The largest boulders are 1 m in diameter and the deposit is clast supported. Flat boulders in this fluvial deposit display imbrication indicating incoming currents from the northeast. The marine sedimentary succession starts with a 1 m-thick torrential deposit (sub-layer 5a). The lower 60 cm correspond to a thinly layered grey sandy deposit with scattered pebbles. The upper 40 cm are intensely bioturbated and contain shells of *S. cuccullata* and moulds of *T. bicingulata*. The dominant galleries are sub-horizontal up to 15 cm in diameter, and fewer, thinner, vertical burrows.

The stratigraphic succession continues with 6–7 m of fine sandstone with ill-defined parallel stratification (sub-layers 5b and 5c). It shows intense bioturbation with *T. suevicus* that shows galleries with horizontal, oblique, and vertical tunnels, ranging in diameter from a few millimetres to 10 cm, and progressively decreasing in intensity towards the top. Some tunnels are branched. The sandstone contains shells of *S. cuccullata*, abundant moulds of *T. bicingulata*, rare shells of *Conus* spp., *T. latus*, *A. opercularis*, and dispersed and poorly preserved rhodoliths mostly concentrated at the basal section of the sequence. The first 1 m (sub-layer 5b) is characterized by the presence of several moulds of *T. bicingulata*, but mainly by the occurrence of articulated shells of *S. senilis* in living position (Fig. 4E). The sedimentary succession presents a lenticular geometry draping over the basaltic basement, which gradually rises to an elevation of 10–11 m above present-day mean sea level (apsl), thus representing the submersion and filling of a palaeotopography (fluvial valley), similar to the present-day topography.

4.2. Sediment characterization

The grain size of the sediment sampled from the fossiliferous stratigraphic succession (samples 1–5) varies from medium to coarse sand, whereas the samples collected from the present-day tidal flats show a variation from fine to medium sand (Table 1). Only sample 6 shows a moderate calibration, with the remaining samples poorly calibrated. The asymmetry of the sampled fossiliferous sediment varies from positive to negative, while the samples from the tidal flat (samples 6–7) present a negative asymmetry. Unlike sample 6, which presents a leptokurtic distribution curve, all remaining samples are platykurtic (Table 1).

Based on Flemming's (2000) textural classification, the sediment of samples 1 and 4 are classified as "slightly sandy mud", samples 3 and 5 as "sandy mud", and sample 2 as "muddy sand", whereas the samples from the tidal flat are "slightly sandy mud" (sample 6) and "slightly muddy sand" (sample 7).

4.3. Fossil and present-day faunal content

The total number of specific molluscan taxa reported for this bay compiled from the literature and including the present results, amounts to 48: 29 reported from the MIS 11 marine sediments and another 29 found on the present-day tidal flat; only ten species are common to both contexts (Table 2).

We excluded from the following analysis the eight specific taxa reported for this outcrop by Serralheiro et al. (1976; Table 2) that we did not find. The only mollusc species having a calcitic shell is the bivalve *Saccostrea cuccullata* (Supplementary Table S1); all other taxa present aragonitic, or a variable combination of aragonitic/calcitic shells. Regarding life habit, most are epifaunal, with only five infaunal species: four bivalves [(*Loripes* cf. *orbiculatus* Poli, 1795, *Megaxinus* sp., *S. senilis*, *Tagelus* cf. *adansonii* (Bosc, 1801)], and one gastropod (*T. bicingulata*). Most of the taxa are mobile, with only one quarter of the species (10 taxa) living attached to the substrate (Supplementary Table S1). Concerning the trophic composition, 16 taxa are grazers, 14 are suspension-feeders (all bivalves), 10 are carnivores, 5 are omnivorous, and only 2 are deposit feeders (Supplementary Table S1). Most of the species (26 taxa) live associated with rocky shores, with fewer living in sandy environments (13), gravel (9) and among algae (6). Of the 40 tropical taxa listed in Supplementary Table S1, about half (22) extend their geographical ranges to subtropical latitudes as well. Finally, when it comes to habitat, all but one species [*Cymbula safiana* (Lamarck, 1819)] are coastal taxa, only 5 and 4 are considered as outer shelf or oceanic taxa, respectively. There are 10 taxa that may live in brackish conditions, and only one, the bivalve *S. cuccullata*, is able to endure hypersaline conditions (Supplementary Table S1).

4.3.1. Fossil samples

The preservation of the fossil specimens is not uniform, with smaller specimens being less well preserved. Representatives of five phyla were collected (Foraminifera, Echinodermata, Mollusca, Arthropoda, and Bryozoa). The Mollusca is the best represented phylum, with 21 specific taxa and 314 specimens (Table 2). The most abundant species are *S. cuccullata* (32.17 %), *S. senilis* (19.75 %), *A. opercularis* (18.15 %), *T. bicingulata* (8.60 %), and *T. latus* (6.05 %), followed by *Thais nodosa* (Linnaeus, 1758) (3.50 %). The remaining species represent 11.78 % of the specimens. The fossil assemblage has a low biodiversity, a fact already mentioned by Serralheiro (1976; Table 2).

Calcareous nannofossils are very rare and poorly preserved, with evidences of dissolution/ recrystallization. They were collected in facies 5b, 6a, and 6b of the marine terrace of Nossa Senhora da Luz Bay (cf. Fig. 2), and are represented by four specific taxa: a small, identified with open nomenclature, *Gephyrocapsa* sp., *Gephyrocapsa caribbeanica* Boudreaux & Hay, 1967, *Gephyrocapsa oceanica* Kamptner, 1943, and *Umbilicosphaera sibogae* (Weber Bosse) Gaarder, 1970.

Layers 4 (Logs A and C, Fig. 2) and 5 (Logs A to D, Fig. 2) show dense bioturbation with *Thalassinoides suevicus*, as well as abundant shells of *S. senilis* showing *Entobia* isp. Bioerosion structures.

4.3.2. Present-day fauna

The present-day fauna samples yielded representatives of four phyla with the Mollusca, again, being the best represented with 29 specific taxa (Table 2). A total of 381 specimens were collected (Table 2). The most abundant species are *Nerita senegalensis* Gmelin, 1791 (26.77 %), *T. nodosa* (16.54 %), and *Gemophos viverratus* (Kiener, L.C., 1834) (13.39 %), followed by *Hipponix* cf. *subrufus* (Lamarck, 1822) (6.04 %), *L.* cf. *orbiculatus* (4.20 %), *Fissurella* sp. (4.20 %), and *T. bicingulata* (3.67

%). The remaining species represent 25.19 % of the specimens (Table 2).

4.4. U/Th disequilibrium geochronology

A total of six coral samples were analysed and all were found to be close to the upper limit of the laser-ablation U—Th dating technique proposed by Niki et al. (2022; cf. Table 3). In samples where Newton-Raphson iterations were able to provide an age uncertainty, resulting coral ages ranged from 383 to 357 ka with a typically uncertainty of ±72 kyrs (2σ). Whilst none of these ages are precise, they do allow us to distinguish these MIS 11 deposits from younger interglacials (e.g. MIS 5e, ~125 ka).

5. Discussion

5.1. Age of the deposit

The transgressive sedimentary succession found at Nossa Senhora da Luz Bay indicates deposition during a sea-level rise and successive highstand, necessarily during an interglacial period as compatible with its stratigraphic position, elevation (in the context of an uplifting island), and degree of preservation. Accordingly, it is reasonable to postulate that this marine terrace was either formed during a time when sea level was higher than the modern sea level, for example MIS 5e or MIS 11c, or during MIS 9e, but that would require very high uplift rates, as maximum sea level during MIS 9e was lower than today (Bintanja et al., 2005; Miller et al., 2011).

The coral samples from the Nossa Senhora da Luz sedimentary succession dated by U/Th disequilibrium geochronology, yielded mean ages of ~370 ka, which fall within the MIS 11 interval (424–374 ka; Lisiecki and Raymo, 2005). These dates suggest that the sedimentary succession at Nossa Senhora da Luz Bay was formed during the MIS 11 interglacial and not during the later MIS 5e sea level highstand at 120 ka. Most of the calcareous nannofossil species present in the sediments of the lower beds of the study site, showing low abundances and diversity as expected for a semi-confined palaeoenvironment like the one found in the present-day bay (Fig. 7), confirm a very coastal facies with an indication of warm waters. The presence of the extinct species *Gephyrocapsa caribbeanica* corroborates that these deposits fall within the *G. caribbeanica* zone that lasted from MIS 14 to MIS 8 (Bollmann et al., 1998; Baumann and Freitag, 2004). Additionally, the absence of *Pseudoemiliania lacunosa* Kamptner, 1963 ex Gartner, 1969 places these sediments younger than MIS 12 (<440 ka; Raffi et al., 2006). Thus, the calcareous nannofossil assemblages, while low in diversity, provide relevant biostratigraphic constrains and support the assignment to MIS 11.

5.2. Stratigraphic succession and palaeoenvironment

The transgressive MIS 11c sedimentary succession at Nossa Senhora da Luz Bay documents the transition from a subaerial environment incised by fluvial valleys, into a confined, sheltered marine bay environment similar to its present-day environment. Sediment analysis (Table 1) shows a variation in grain size distribution, with the present-day tidal flat sediments being better calibrated than the MIS 11c ones. Moreover, MIS 11c deposits are slightly coarser, suggesting that wave energy inside the bay was higher during the MIS 11c than it is today.

The sedimentary succession starts with conglomerate and breccia deposits resulting from fluvial discharge (Logs A, C and D). Today (and during MIS 11) the bay is the mouth of two main streams (Fig. 5). The tropical climate in Cabo Verde is characterized by rare, short but intense periods of precipitation, resulting in a torrential regime (Costa and Nunes, 2008; Varela-Lopes et al., 2014). These intermittent, torrential rains feeding the streams that drain mainly into the southern side of Nossa Senhora da Luz Bay are probably the reason for the absence of fossiliferous marine sediments on the south side of the bay (Fig. 5), most likely having been eroded away.

The presence of a paleosol (sub-layer 2b, Logs A and C, Fig. 2) developed on top of a marine conglomerate implies a relative sea-level fall producing emersion and interruption of sedimentation for a period long enough to allow pedogenesis. A subsequent relative sea-level rise event submerged the paleosol and led to suitable ecological conditions for the later settlement of a monospecific initial oyster bank, composed almost entirely of articulated shells of the bivalve *S. cucullata* (sub-layer 3a in Log A; Figs. 2, 3C). Monospecific oyster banks are known to occur in river mouths and estuaries, being associated with the early transgressive systems tract, when pre-existing topographies were flooded by sea-level rise, providing ecological conditions suitable for the establishment of dense oyster clusters (Pufahl and James, 2006). The higher matrix content in sub-layers 3b and 3c (Log A, Fig. 2), as well as the occurrence of disarticulated valves of oysters, suggesting post-mortem transport, and the presence of boulders and coarse sediment in sub-layer 3c, suggest an increase in stream discharge that we relate to torrential rain events.

The higher biodiversity recorded in layer 4 (Logs A and C; Fig. 2), as well as the higher bioturbation, show that more marine species inhabited the bay (e.g. corals). The first specimens of the bivalve *S. senilis* also begins to appear in the targeted sedimentary succession.

The thick package of fine silty-clay sediment in layer 5 is characterized by horizontal to sub-horizontal laminar stratification, suggesting a calm, low energy, environment. In Log A, the lower layers of this sedimentary succession exhibit desiccation cracks indicating a shallow environment temporarily exposed to subaerial conditions. This bed is intensely bioturbated, displaying a dense network of burrows (sub-layer 5b, Fig. 3B) throughout its entire vertical extension (Fig. 2). The grain size and thickness of this bed show that, for an extended period, only fine sediment was transported into the bay, suggesting the presence of a wide low-energy tidal flat similar to the present-day conditions in the inner part of Nossa Senhora da Luz Bay. This type of ecosystems is usually highly biodiverse in meiofauna (Dittmann, 2000, and references therein; Schratzberger and Ingels, 2018). Crustaceans and polychaetes are usually responsible for most of the burrows (e.g., *Thalassinoides suevicus*). Ichnofossil records from insular environments are known from other Macaronesian islands, with several examples of galleries made by polychaetes, crustaceans and echinoderms: e.g., *Macaronichnus segregatis* Clifton & Thompson, 1978, *Palaeophycus* isp., and *Diopatrichnus santamariensis* Uchman, Quintino & Rodrigues, 2017, produced by polychaetes (Santos et al., 2015; Uchman et al., 2016, 2017, 2018, 2020); *Thalassinoides* isp., *Ophiomorpha nodosa* Lundgren, 1981, and *Centrichnus dentatus* Uchman, Wisshak, Madeira, Melo, Sachcetti, Ávila, G. & Ávila, S., 2025, produced by crustaceans; *Bichordites monastiriensis* Plaziat & Mahmoudi, 1988, *Circolites kotoucensis* Mikuláš, 1992, and *Ericichnus bromleyi* Santos & Mayoral, 2015, produced by echinoderms (Santos et al., 2015; Ávila et al., 2023). Some of these burrowing organisms are represented by body fossils, such as spines of the *Eucidaris* echinoid and claws of unidentified decapod crustaceans, but possibly also by several molluscs such as *T. bicingulata* and *S. senilis*. The latter two species are abundant in sub-layer 5d, where remains of *S. senilis* in living position, as well as several casts of *T. bicingulata,* are found (Fig. 4E and F).

5.3. Crustaceans as 'ecosystem engineers'

An ecosystem engineer is an organism that modifies, creates or destroys habitat and directly or indirectly modulates the availability of resources to other species, "causing physical state changes in biotic or abiotic materials" (Jones et al., 1994) and can be classified as autogenic (changing the environment via their own physical structures) or allogenic (changing the environment by transforming living or non-living materials from one physical state (e.g., living trees in a forest) to another (e.g., dead trees in a beaver dam) via mechanical or other actions). Crustaceans are allogenic engineers and play an important role in

shaping the ecosystems. Crustacean burrows are one of the most pervasive changes performed by these organisms. These structures result, e.g., from the need of refuge for hot and dry periods (Kristensen, 2008, and references therein), and can also function as habitat for other species. Several crab claws (that will be the subject of a forthcoming paper) attest to the presence of decapod crustaceans in the bay at least since the MIS 11. The thickness of the sedimentary succession and the complex network of galleries (layer 5, Logs A–D) suggest a high sedimentation rate and an intense crab activity.

5.4. The importance of rhodolith beds

One of the most distinctive layers of the MIS 11 sedimentary succession in Nossa Senhora da Luz Bay is the thick rhodolith deposit in layer 6 (Logs A and B; Fig. 2). Rhodolith beds are rare and fragile ecosystems (Wilson et al., 2004; Joshi et al., 2017) and their preservation in the fossil record is relatively uncommon (see Silva et al., 2019; Uchman et al., 2020), with most examples corresponding to more resistant assemblages of lumpy rhodolith morphologies. And, notwithstanding the fact that Macaronesia exhibits several remarkable examples of well-preserved fossil rhodolith beds (e.g., Johnson et al., 2011, Johnson et al., 2017; Rebelo et al., 2016, 2021, 2022, 2025), these mostly correspond to hard-wearing lumpy forms, denoting their higher energetic formational and depositional environment. The rhodolith bed of Nossa Senhora da Luz, however, stands out on account of the exceptional degree of preservation of its very large (up to 15 cm in diameter), extremely fine-branching – and hence very fragile – rhodoliths; these are largely unbroken and are stacked on top of each other forming a layer that reaches up to 3 m in thickness. This layer is thus, arguably, one of the better-preserved calm-water fragile fossil rhodolith assemblages in the fossil record of the Atlantic, and a testimony to the degree of protection afforded by the Nossa Senhora da Luz Bay during the sea-level highstand during which it was formed, as well as during subsequent highstands. Moreover, rhodolith beds are known to require constant submergence (Barbera et al., 2003). Thus, assuming a sea level rise of 6–13 m during the MIS 11c (Raymo and Mitrovica, 2012), the only sites suitable for rhodolith development would be those recorded at the top of layer 5, located 4–5 m apsl (Logs A and B, Fig. 2).

Rhodolith beds are important ecosystems that provide three-dimensional habitats for a highly diverse suite of organisms (Fig. 6), including epibenthic, epiphytic, cryptic, and infaunal species (Birkett et al., 1998; Steller et al., 2003; Basso and Brusoni, 2004; Grall et al., 2006; Amado-Filho et al., 2007), especially crustaceans and polychaetes (Harvey and Bird, 2008). Being a delicate ecosystem, its presence helps on the reconstruction of palaeoenvironments (Bassi et al., 2012). Rhodolith beds are known to occur in a variety of temperatures, withstanding temperatures as low as 2 °C [e.g., *Phymatolithon calcareum* (Pallas) Adey and McKibbin, 1970], and tend to occupy high salinity areas (Bosence, 1976). The coralline algae that form the rhodoliths are light dependent, so they only occur within the euphotic zone (Birkett et al., 1998). They require enough wave action and/or bioturbation to promote rotation and do not tolerate emersion and desiccation (Barbera et al., 2003). Therefore, they tend to occur in sheltered areas, such as coastal bays or inlets (Bosence, 1979) presenting an optimal wave action to prevent the burial of the thalli (Joshi et al., 2017) by high sedimentation rates (Rebelo et al., 2022). The rhodolith bed at Nossa Senhora da Luz Bay represents an extremely fragile stack of very fine-branching rhodoliths, most probably still in their life position, denoting a relatively calm environment, possibly under fairly constant wave energy conditions, as the one afforded by an inlet well protected by rocky spurs on both sides, which would moderate, by refraction, the wave energy entering the inlet (see Fig. 7B).

The rhodolith bed (layer 6) is recorded at the top unit of Logs A and B. Since this unit does not exhibit any terrigenous sediments in its matrix, we infer that the rhodolith bed was not affected by inland sediment discharges and attribute its preservation to subsequent emersion caused by a relative sea-level fall. The rhodolith bed also indicates low turbidity during the final recorded stages of the MIS 11c sedimentary succession at the study site, in contrast with present-day conditions (cf. Supplementary material 3). Such conditions would indicate that the rhodolith bed was formed towards the end or after the North African humid period (420–405 ka; see Helmke et al., 2008; Grant et al., 2022), when northward heat flux in the North Atlantic was at its maximum and SSTs were warmest throughout the Atlantic basin (Stein et al., 2009; Voelker et al., 2010; Rodrigues et al., 2011; Milker et al., 2013; Hu et al., 2024).

5.5. Inferring vertical land movement rates at Nossa Senhora da Luz Bay

Eustatic oscillations (Haq et al., 1987; Bintanja et al., 2005; Miller et al., 2005, 2011; Kominz et al., 2008) allied to uplift resulted in considerable topographic changes in Santiago Island, which are more noticeable in flat and gently dipping coastal areas such as the Nossa Senhora da Luz Bay region.

Like other Macaronesian islands [e.g., Santa Maria Island, Azores (Ramalho et al., 2017); Madeira Island (Ramalho et al., 2015a); Lanzarote, Fuerteventura, Tenerife, and La Gomera, in the Canaries (Acosta et al., 2003 and references therein)], Santiago has a complex vertical movement history, either dominated by a general uplift trend, or including significant uplift episodes (Ramalho et al., 2010a, 2010b, 2010c; Marques et al., 2020). For Santiago, Ramalho et al. (2010b, 2010c) estimated a long-term, averaged uplift rate of 100 m/Myr for the last 4 Ma.

As described by Ramalho (2011), the vertical displacement can be calculated by:

$$D_v = h + d – H$$

where D_v corresponds to the vertical displacement due to land movement, h is the present elevation, d the inferred palaeodepth of sea water, and H the contemporaneous palaeo-global mean sea-level (PGMSL) height (all measured in meters). In the calculation of the vertical displacement of Santiago presented herein, we implicitly included glacial isostatic adjustments into *Dv*, which is not entirely adequate, as glacial isostatic adjustments follows glacial cycles, while *Dv* represents a trend through time. The msl height for MIS 11c (= +8 m) was obtained from Miller et al. (2011). For Nossa Senhora da Luz Bay and using the data for the MIS 11c maximum ($H = +8$ m at circa 405 kyr), $Dv = 40.5$ m (estimated uplift rate of 100 m/Ma x 0.405 Ma), and $h = 0$ m, we obtain a value for d of +48.5 m (Fig. 8). If we use other sea level curves (e.g., Raymo and Mitrovica, 2012), MIS 11c maximum PGMSL values range from +6 to +13 m, which translates into values for d ranging from +46.5 to +53.5 m. Thus, we should expect to find the MIS 11c marine terraces at these altitudes. However, no signs of such terraces were found.

The existence of several raised marine terraces in Cabo Verde is documented since Serralheiro (1976), with fossiliferous sequences at Nossa Senhora da Luz Bay positioned at 2–4 m, 5–10 m and at 15–25 m apsl. Our data supports the interpretation that only those at +2–4 m and + 5–10 m correspond to MIS 11c fossiliferous deposits, whilst the ones standing 15–25 m apsl are interpreted as a younger tsunami deposit (Ramalho et al., 2015b; Ávila et al., 2017, 2025). The MIS 11c deposits were found at a maximum altitude of 12 m apsl (at the location of Log D), where specimens of *S. senilis* are found in living position. This infaunal bivalve is known to tolerate periodic emersion during low tide (Lavaud et al., 2013). Therefore, because of higher sea-level during MIS 11c and vertical displacement due to the recorded uplift trend, the application of Ramalho's (2011) vertical displacement formula results in a value of $D_v = 4$ m (i.e., 0,01 mm/yr; $h = 0$, $d = 12$ and $H = 8$ m). This value indicates a variable uplift rate in Santiago (as already suggested by Marques et al., 2020), with a significantly slower uplift during the last ~400 ka. Changes in uplift trends are not uncommon in oceanic islands and have also been reported from other islands in the archipelago (Ramalho et al., 2010b, 2010c; Madeira et al., 2010), and from Santa Maria Island in the Azores (Ricchi et al., 2020). These observations,

Table 3
U/Th disequilibrium ages for Nossa Senhora da Luz corals. * Newton-Raphson iterations did not converge on an uncertainty for this sample.

Sample code	Latitude	Longitude	U/Th age (ka) ± 2σ
ST84–1	15.04407°N	23.45088°W	**378 ± 65**
ST84–3	15.04407°N	23.45088°W	373 ± 72
ST85–1	15.04293°N	23.45122°W	371 ± 75
ST86–1	15.04377°N	23.45175°W	357 ± 83
STG34–2	15.04310°N	23.45130°W	**383 ± 66**
STG34–4	15.04310°N	23.45130°W	323*

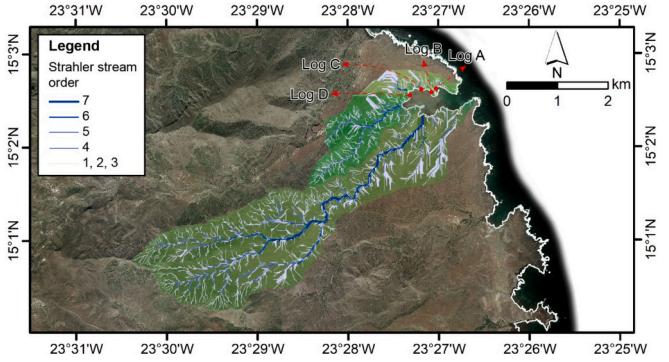

Fig. 5. Hydrographic basin of Nossa Senhora da Luz Bay. Green areas represent hydrographic basins. Stream order was measured according to the Strahler (1952) method. The main stream has an order of 7 (at the scale used) and is represented in dark blue. (For interpretation of the references to colour in this figure legend, the reader is referred to the web version of this article.)

however, are at odds with the much faster uplift rate proposed by Marques et al. (2020) of 0.14 mm/yr in the last ~800 ka, showing that more research is necessary to reconcile vertical motion rates derived from lava deltas with those obtained from marine terraces.

5.6. Palaeoclimatology and palaeoecology

Only ten species of invertebrates are common to both the middle Pleistocene fossil assemblage and the present-day fauna at Nossa Senhora da Luz Bay (eight gastropods and two bivalves; cf. Table 2). Moreover, at least two bivalve species reported for the MIS 11c of Cabo Verde are thought to have disappeared from the archipelago, namely *Saccostrea cucullata* and *Senilia senilis*.

In the Atlantic coasts of Africa, the extant oyster *S. cucullata* has a geographic distribution ranging from the Ivory Coast down to Angola (Cosel and Gofas, 2019). It has also been reported from the Indian Ocean (Dye, 1989) and the south-eastern and southern Brazilian coasts (Amaral et al., 2020). This species inhabits brackish water environments, being common at river mouths and estuaries (Awati and Rai, 1931; Montesinos, 2011). In the Macaronesia geographic region, *S. cucullata* has been reported from the MIS 11c of the Canary Islands (Montesinos, 2011; Montesinos et al., 2014) and from Quaternary marine fossiliferous deposits of Santiago Island (Serralheiro, 1976).

Today, the infaunal bivalve *S. senilis* occurs along the coasts of West Africa, from Western Sahara to Angola (Cosel and Gofas, 2019), living in silty sand bottoms in coastal lagoons and channels, and brackish tidal flats (Djangmah et al., 1979; Wolff et al., 1987; Lavaud et al., 2013), tolerating a range of temperatures from 16° to 31 °C (Debenay et al., 1994). Cosel (1982) and Cosel and Gofas (2019) report extant *S. senilis* from Cabo Verde. However, according to Rui Freitas (pers. comm. 2019) no live specimens were ever collected in the archipelago, only a few disarticulated valves. If *S. senilis* did occur in the archipelago today, being an edible mollusc, it would have been harvested, as it is in Mauritania (Lavaud et al., 2013). Therefore, we consider *S. senilis* to be absent in present-day Cabo Verde. Fossil occurrences of *S. senilis* in the Macaronesian region have been reported only from Quaternary marine terraces of Santiago and tsunami deposits in Maio in Cabo Verde (Serralheiro, 1976; Madeira et al., 2020).

Both *S. senilis* and *S. cucullata* live in brackish water environments, typical of river mouths, estuaries, and coastal lagoons. Presently, the MIS 11c marine fossiliferous sequences exposed at Nossa Senhora da Luz Bay cover ~0.035 km^2, a very restricted area when compared to the current area of the bay (0.53 km^2) and its inferred area during the MIS 11c peak (1.16 km^2; Fig. 7; see point 5.1. for discussion about erosion). A coastal lagoon still exists today at Nossa Senhora da Luz Bay, however, the current low precipitation regime in Santiago Island (Varela-Lopes & Molion, 2014) prevents the occurrence of suitable ecological conditions for the existence of populations of *S. cucullata* and *S. senilis* there.

For the Last Interglacial (MIS 5e, i.e., 129–115 ka; Shackleton et al., 2020), Hansen et al. (2015) and Hearty et al. (2017) inferred stormier climatic conditions, which would produce a more humid tropical environment. The presence of *S. cucullata* and *S. senilis* at the Nossa Senhora da Luz Bay fossiliferous sequence, coupled with their absence today, suggests that the environmental conditions during the MIS 11c were closer to the ones during the MIS 5e. Higher precipitation during MIS 11c occurred during the insolation maxima when the NW African monsoon was intensified leading to wetter conditions (increased river run-off) between 420 and 405 ka (Helmke et al., 2008; Grant et al., 2022; O'Mara et al., 2022).

5.7. Palaeobiogeographical relevance

The studied fossiliferous sequence provides valuable clues on marine life in Cabo Verde during the middle Pleistocene. In stark contrast to Spalding et al. (2007), who considered the present-day faunas of Cabo Verde as representing an ecoregion, Freitas et al. (2019) viewed them as an autonomous biogeographic subprovince. This reclassification from ecoregion to subprovince was based on the high number of endemic Cabo Verdean species belonging to several marine phyla (Freitas et al., 2019). A similar analysis has also been made for the late Pleistocene (MIS 5e; Melo et al., 2023), showing a different situation: whereas today the Webbnesia (including the Madeira, Selvagens, and Canaries archipelagos; Freitas et al., 2019) is ranked as an ecoregion and Cabo Verde as a subprovince, both acting as different marine biogeographic entities, data shows that during MIS 5e a closer biogeographic relationship between the marine faunas of Cabo Verde and those of the Canary archipelagos existed (Melo et al., 2023)). The biogeographic relationships between them during the MIS 5e were quite different from what is seen today, stressing the need for further biogeographic studies of past interglacials, namely MIS 11c.

The geographical range of the specific taxa reported from the MIS 11c fossiliferous record, and the present-day fauna of Nossa Senhora da Luz was checked, based on unpublished data provided by one of the authors (S.P. Ávila). The data was computed, resulting in the dendrogram presented in Fig. 9. Three groups are statistically valid and stand out from this analysis: 1) GME (Gulf of Mexico) and CAR (Caribbean Sea); 2) NAF [NW African shores, including Atlantic Morocco, from the Straits of Gibraltar south to Western Sahara, Mauritania, and Senegal]; PRE (Holocene fauna collected within the Nossa Senhora da Luz Bay); and CAB (Cabo Verde Archipelago); and 3) AZO (Azores); POR (western Atlantic Iberian façade from Cabo Vilán, western Galician shores, down to Cape São Vicente, and southern shores of Algarve, Portugal); MED (Mediterranean Sea); CAN (Canary Islands); SEL (Selvagens); and MAD (Madeira, Porto Santo, and Desertas Islands).

Interestingly, despite the low statistical relevance, the assemblage reported for MIS 11c at Nossa Senhora da Luz Bay shows a closer biogeographical similarity with the present-day faunas of SAF (SW African shores, from Senegal to Angola). This higher similarity with Senegal highlights the fact that some MIS 11c species that were subsequently extirpated from the Cabo Verde archipelago occur today on the

coast of Senegal. As mentioned by Melo et al. (2023), the extirpation of species from Cabo Verde stresses the need for studies focusing on the ecological factors that control species distribution in this region.

For the northern Macaronesian archipelagos, changes in mean SST have been widely used to explain the extirpation of thermophilic species during the MIS 5e. However, climatic conditions in Cabo Verde during the Quaternary have always been tropical (Ávila et al., 2016a; Melo et al., 2022a). Moreover, other factors, such as climatic stability (which correlates with latitude and promotes low extinction rates) and high littoral area values during interglacials, both promoting high speciation rates, explain why Cabo Verde faunas show high endemism, including SIME (Single Island Marine Endemics), an extremely rare situation in the marine realm. These variables and their effect on insular shallow-water ecosystems were fully explored by Ávila et al. (2019) and their Sea-Level

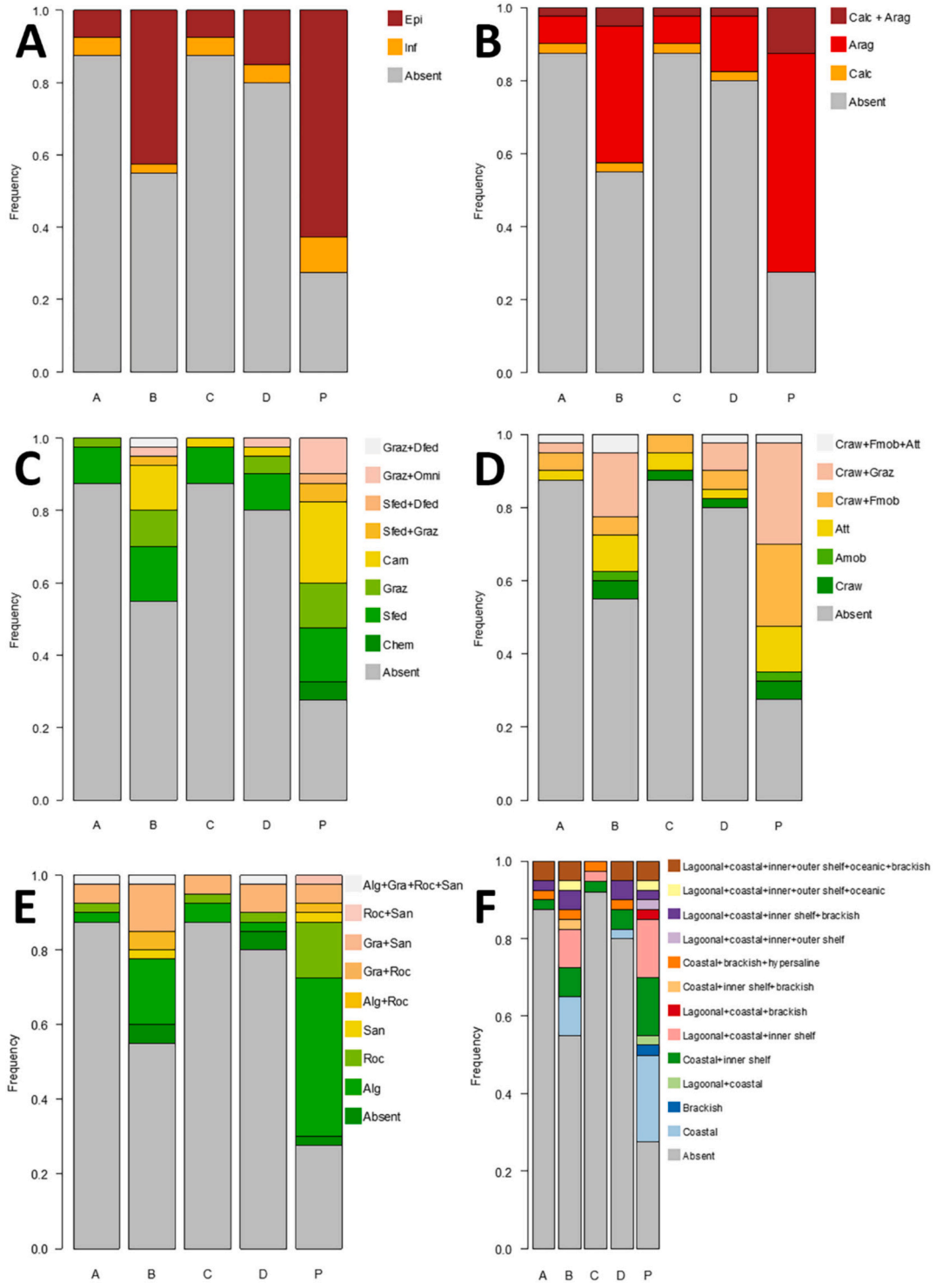

Fig. 6. Functional groups comparisons among the MIS 11c samples (Logs A, B, C, and D) and the present ones (P). A: Life habitat (epifaunal, infaunal). B: Shell composition (aragonite, calcite). C: Diet (grazer, deposit feeder, omnivore, suspension feeder, chemosymbiotic). D: Type of locomotion (crawler, facultatively mobile, actively mobile, attached).
Absent: no information was obtained for the analysed functional trait.

Sensitive dynamic model of marine island biogeography.

Physical barriers (e.g., upwelling systems) are currently present between the Cabo Verdean islands and Senegal, thus preventing the migration/dispersal of shallow-water marine species between the archipelago and the nearby African coastal areas (Capet et al., 2017). Upwelling appears, however, to have been diminished during the early phase of MIS 11 and more seasonal (see Fig. 6 in Milker et al., 2013), also supported by the decreased Saharan dust flux in the Cabo Verde region (Crocker et al., 2022). Similar to glacial Termination II and MIS 5e (Ávila et al., 2019; Melo et al., 2022a), we postulate that the North Atlantic meltwater event during Termination V (430–425 ka; e. g., Stein et al., 2009; Rodrigues et al., 2011), followed by an expanded period with diminished winds during the African Humid period (Helmke et al., 2008; Crocker et al., 2022), severely impacted the Canary Current / Cabo Verde Frontal Zone and Senegal Upwelling Centre, effectively causing these physical barriers to nearly disappear. Northward transport of tropical planktonic foraminifera species during the transition from MIS 12 into early MIS 11c was observed by Voelker et al. (2010) on the western Portuguese margin, potentially linked to a northward transport along the NW African margin, and is also seen during the MIS 10 to interglacial MIS 9e transition (A. Voelker, unpublished data). Consequently, the increase in the number of mollusc species and specimens exchanged between Cabo Verde islands and Senegal is probably linked to the climatic conditions preceding and during MIS 11c and potentially MIS 9e, the two middle Pleistocene periods associated with a postulated stronger North Equatorial Current and an intensification of the subtropical gyre circulation (Billups et al., 2020).

5.8. *Pleistocene interglacials in the Cabo Verde Archipelago: comparing MIS 11c with MIS 5e deposits*

The two warmest Quaternary interglacials (MIS 11c and MIS 5e) share similarities that make it difficult to differentiate their sedimentary record. Being one of the longest interglacials (27 kyr in duration; Tzedakis et al., 2012), the MIS 11c fossiliferous sequences are usually thicker than MIS 5e counterparts. However, MIS 11c fossiliferous

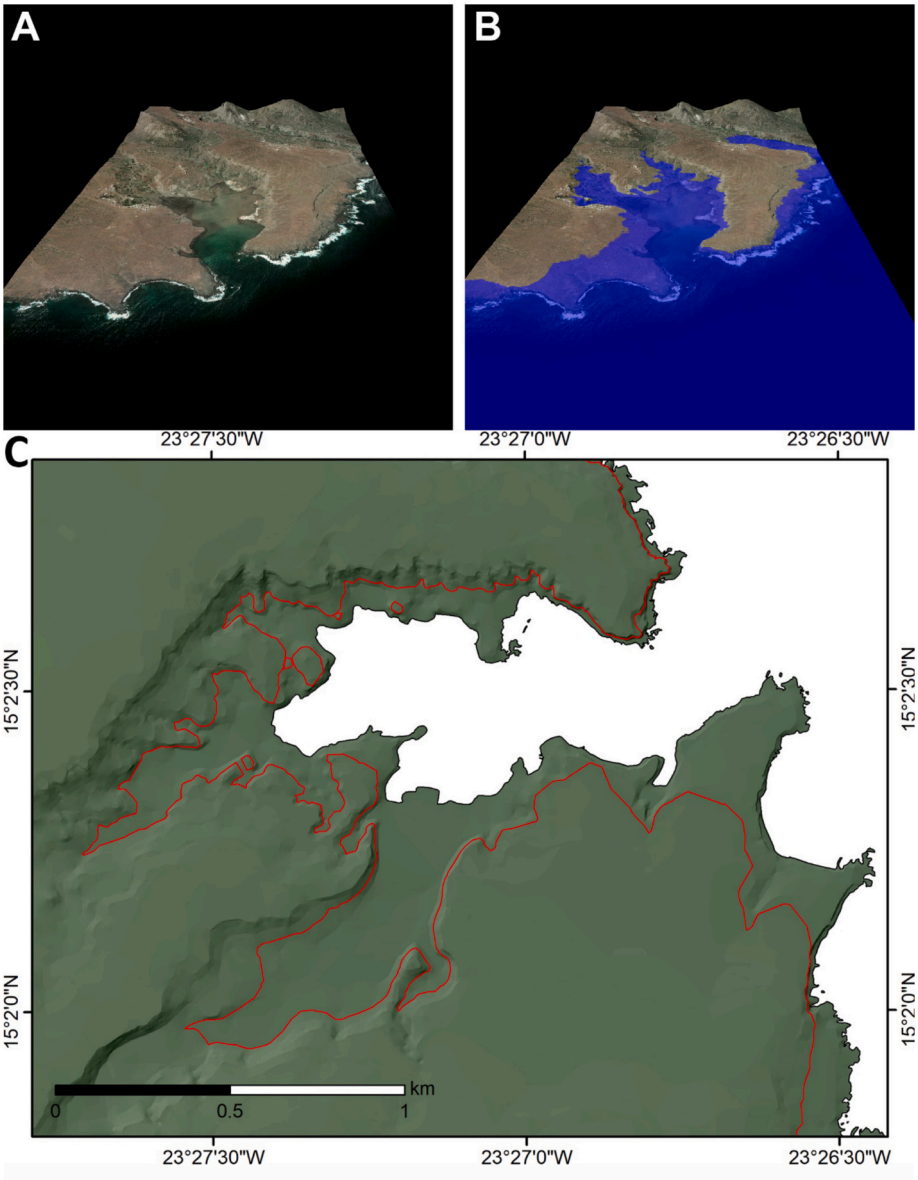

Fig. 7. 3D view of Nossa Senhora da Luz Bay. A: Present-day geographical configuration of the bay; B: Inferred geographical configuration of the bay during MIS 11c, with the sea level 8 m higher than present msl. C: The red line represents the estimated position of sea level during MIS 11c. Altimetric data retrieved from DEM (2010). (For interpretation of the references to colour in this figure legend, the reader is referred to the web version of this article.)

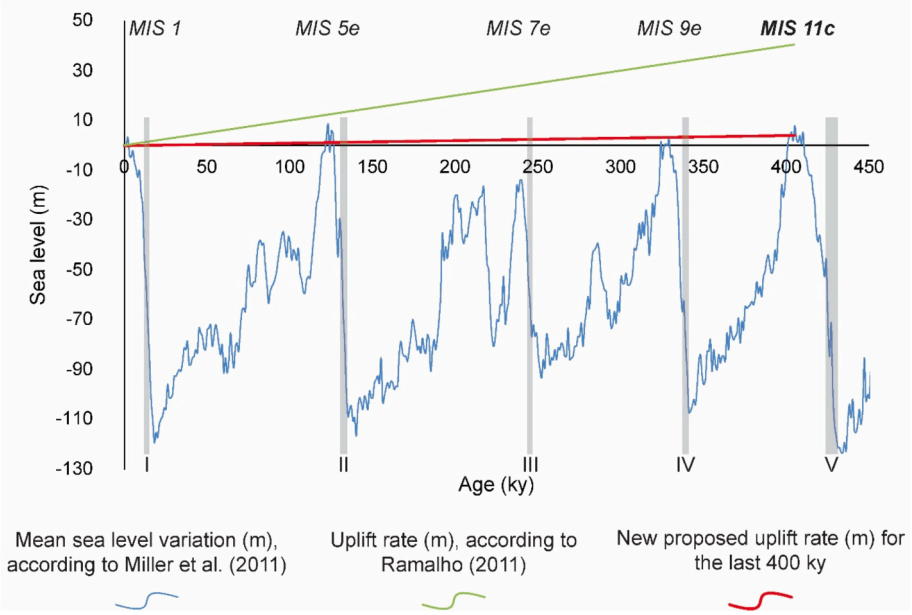

Fig. 8. Reconstruction of Santiago Island uplift. The green line represents the uplift rate suggested by Ramalho (2011) of 100 m/Ma; the red line represents the uplift rate of 10 m/Ma proposed herein. Mean sea level variation for the last 450 kyr from Miller et al. (2011; blue line); marine isotopic stages and terminations according to Railsback et al. (2015). (For interpretation of the references to colour in this figure legend, the reader is referred to the web version of this article.)

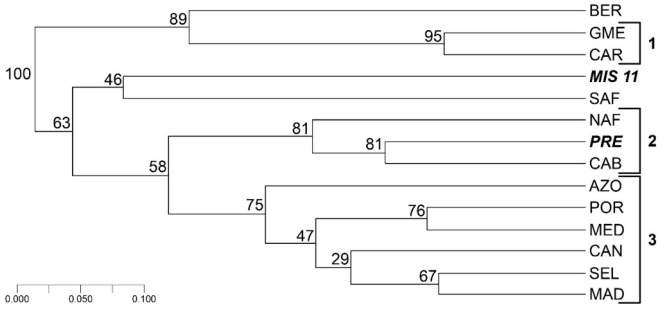

Fig. 9. Dendrogram depicting the biogeographic similarity between the marine molluscan assemblage in the study outcrop and the faunas of several present-day Atlantic regions (29 species in total). Non-bold numbers correspond to the bootstrap values providing support for each tree node (100 repetitions of 100 trees). Numbers in bold represent the clusters validated by Mantel statistics (Pearson). BER (Bermuda); GME (Gulf of Mexico); CAR (Caribbean Sea); MIS 11c (MIS 11c marine terrace from Nossa Senhora da Luz Bay); SAF (SW African shores, from Senegal to Angola); NAF [NW African shores, including Atlantic Morocco, from Straits of Gibraltar south, Western Sahara, Mauritania, down to Cape Vert (Senegal)]; PRE (Holocene fauna collected within the Nossa Senhora da Luz Bay); CAB (Cabo Verde Archipelago); AZO (Azores); POR (western Atlantic Iberian façade from Cabo Vilán, western Galician shores, down to Cape São Vicente, and southern shores of Algarve, Portugal); MED (Mediterranean Sea); CAN (Canary Islands); SEL (Selvagens); and MAD (Madeira, Porto Santo, and Desertas Islands).

assemblages are poorly documented throughout the Macaronesian archipelagos, known only from three other locations (cf. section 1). All these deposits are found at altitudes of 10 to 13 m apsl. By contrast, MIS 5e fossiliferous outcrops have been reported for the Azores (Santa Maria Island; Ávila et al., 2002, 2008, 2009a, 2010; Madeira et al., 2011; Ávila et al., 2015a, 2015b, 2018a, 2020; Hyzny et al., 2021), Madeira (Porto Santo Island; Gerber et al., 1989), Selvagens (García-Talavera and Sánchez-Pinto, 2001), Canaries (Meco, 1977, 1981; Meco et al., 1997, 2002; García-Talavera, 1999; Cabero, 2009; Cabero et al., 2010; Montesinos et al., 2014; Martín-González et al., 2016, 2018, 2019), and Cabo Verde (García-Talavera, 1999; Zazo et al., 2010), at altitudes that range from 2 to 3 m apsl (Azores, Canary Islands, and Cabo Verde; Zazo et al., 2002; Ávila et al., 2009a, 2010; Zazo et al., 2010) to a maximum of 7 m apsl (Azores; Ávila et al., 2015a).

Both MIS 11c and MIS 5e Macaronesian fossiliferous sequences are characterized by tropical species that arrived to the different archipelagos either during the final phase of glacial Termination V and II, respectively, or during the MIS 11c and MIS 5e interglacials (Meco et al., 2002; Ávila, 2005; Ávila et al., 2009a; Muhs et al., 2014; Ávila et al., 2015a; Melo et al., 2022a, 2022b), and that were subsequently extirpated during the following glacial episodes (MIS 10 and MIS 5d-2, respectively). The bivalves *Saccostrea cucullata* and *Senilia senilis* are good examples for MIS 11c, whereas *Tethystrombus latus* and several *Conus* spp. better characterize MIS 5e deposits. We stress that, unlike for the remaining Macaronesian archipelagos, for Cabo Verde there is no evidence suggesting a high biotic turnover in the molluscan fauna either during or after MIS 11c, or during MIS 5e, making it difficult to use "ecostratigraphic indicators" (sensu Melo et al., 2022a) for this archipelago.

6. Conclusions

Thick coquina deposits are extremely rare in volcanic oceanic islands. Nossa Senhora da Luz Bay constitutes one of the best-preserved Pleistocene marine fossiliferous sedimentary successions in all Macaronesia, providing unique clues on past climates and how the present interglacial may evolve as a result of climate change and what effects it could have on the Macaronesia geographical region. Moreover, our study suggests that:

1. The fossiliferous sequence exposed at Nossa Senhora da Luz Bay is of MIS 11c age, one of the few sedimentary successions assigned to this interglacial in the context of the Macaronesian archipelagos;
2. The elevation of the MIS 11c deposit at Nossa Senhora da Luz suggests that Santiago, in the last ~400 kyr, experienced an uplift rate of just 0.01 mm/yr, which is much slower than the long-term averaged uplift rates of 0.10 mm/yr proposed by Ramalho et al. (2010a, 2010b, 2010c) and especially that of 0.14 mm/yr proposed by Marques et al. (2020).

3. The MIS 11c fossiliferous sedimentary succession at Nossa Senhora da Luz Bay indicates tropical climatic conditions moister and warmer than those on the island at present;
4. After the MIS 11c interglacial, the ecological conditions at Nossa Senhora da Luz Bay changed (e.g., less discharge of fresh-water into the bay; narrow inlet; higher turbidity of the sea water inside the bay), as the representative MIS 11c species (*S. cuccullata* and *S. senilis*) do not occur today, neither in the bay nor in the archipelago.

Finally, this study provides further insight on what can be expected in the Macaronesia geographical region with future climatic change. If this paleo analogue holds, it is likely this region will experience more tropical conditions, warmer surface oceanic waters, more humid conditions and increased freshwater inputs. These changes will ultimately contribute to the migration of tropical species to higher latitudes, as a result of specific climatological and oceanographical conditions ("windows of opportunity") and possibly follow similar patterns as those presented by Melo et al. (2022a) for MIS 5e.

Declaration of competing interest

The authors declare that the research was conducted in the absence of any commercial or financial relationships that could be construed as a potential conflict of interest.

Acknowledgments

We thank Unidade de Coordenação do Cadastro Predial (UCCP) from Ministério do Ambiente, Habitação e Ordenamento do Território, Cabo Verde, for providing us with the aerial photography and altimetric information from Santiago Island. C.S. Melo benefited from a PhD grant M3.1.a/F/100/2015 from the Regional Government of the Azores. A.C. Rebelo benefited from a Post-Doc grant SFRH/BPD/117810/2016 by FCT – Fundação para a Ciência e a Tecnologia I.P. R. Ramalho acknowledges his "Investigador FCT" contract IF/01641/2015, funded by FCT. AR acknowledges support by the European Research Council (ERC) under the European Union's Horizon 2020 research and innovation programme (grant agreement n. 802414). SPA and PM acknowledge their contracts with project M1.1. A/ INFRAEST CIENT/A/001/2021 - Base de Dados da PaleoBiodiversidade da Macaronésia, funded by the Regional Government of the Azores. SPA appreciates his current FCT/2023.07418 CEEECIND research contract with BIOPOLIS (https://doi.org/10.54499/2023.07418.CEECIND/CP2845/CT0001). AV acknowledges Portuguese national funds from FCT through projects UIDB/04326/2020 (DOI:10.54499/UIDB/04326/2020) and LA/P/0101/2020 (DOI:10.54499/LA/P/0101/2020). This work was partially supported by project PTDC/CTA-GEO/28588/2017 - LISBOA-01-0145-FEDER-028588 UNTIeD, co-funded by the European Regional Development Fund – ERDF, through Programa Operacional Regional de Lisboa (POR Lisboa 2020), and by FCT. This work also benefited from FEDER funds, through the Operational Program for Competitiveness Factors – COMPETE, and from National Funds, through FCT (UID/BIA/50027/2013, UIDB/50027/2020, POCI-01-0145-FEDER-006821), as well as through the Regional Government of the Azores (M1.1.a/005/Funcionamento-C-/2016, CIBIO-A; M3.3.B/ORG.R.C./005/2021, M3.3.B/ORG.R.C./008/2022/EDIÇÃO 1, M3.3.G/EXPEDIÇÕES CIENTÍFICAS/005/2022 and M3.3.G/EXPEDIÇÕES CIENTÍFICAS/004/2022). Finally, this work was also supported by FEDER funds (in 85 %) and by funds from the Regional Government of the Azores (15 %) through the Azores 2020 Operational Program under the VRPROTO project: Virtual Reality PROTOtype: the geological history of "Pedra-que-pica": ACORES-01-0145-FEDER-000078. FCT project UID/GEO/50019/2013 to Instituto Dom Luiz contributed to field-work costs. JM and CMS acknowledge the Portuguese Fundação para a Ciência e a Tecnologia (FCT) I.P./MCTES through national funds (PIDDAC) – UIDB/50019/2020 (https://doi.org/10.54499/UIDB/50019/2020), UIDP/50019/2020 (https://doi.org/10.54499/UIDP/50019/2020) and LA/P/0068/2020 (https://doi.org/10.54499/LA/P/0068/2020).

Appendix A. Supplementary data

Supplementary data to this article can be found online at https://doi.org/10.1016/j.palaeo.2025.113505.

Data availability

The authors confirm that all data necessary for supporting the scientific findings of this paper have been provided.

References

Acosta, J., Uchupi, E., Muñoz, A., Herranz, P., Palomo, C., Ballesteros, M., ZEE Working Group, 2003. Geologic evolution of the Canarian Islands of Lanzarote, Fuerteventura, Gran Canaria and La Gomera and comparison of landslides at these islands with those at Tenerife, La Palma and El Hierro. Mar. Geophys. Res. 24, 1–40.

Adey, W.H., McKibbin, D.L., 1970. Studies on the maerl species *Phymatolithon calcareum* (Pallas) nov. comb. and *Lithothamnion corallioides* Crouan in the Ria de Vigo. Bot. Mar. 13, 100–106.

Amado-Filho, G.M., Maneveldt, G., Manso, R.C.C., Marins, B., Pacheco, M.R., Guimarães, S.M.P.B., 2007. Structure of rhodolith beds from 4 to 55 meters deep along the southern coast of Espírito Santo State, Brazil. Cienc. Mar. 33, 399–410.

Amano, K., 2004. Biogeography and the Pleistocene extinction of neogastropods in the Japan Sea. Palaeogeogr. Palaeoclimatol. Palaeoecol. 202 (3–4), 245–252.

Amaral, V.S., Simone, L.R.L., Tâmega, F.T.S., Barbieri, E., Calazans, S.H., Coutinho, R., Spotorno-Oliveira, P., 2020. New records of the non-indigenous oyster *Saccostrea cucullata* (Bivalvia: Ostreidae) from the southeast and south Brazilian coast. Reg. Stud. Mar. Sci. 33, 100924.

Ávila, S.P., 2005. Processos e Padrões de Dispersão e Colonização nos Rissoidae (Mollusca: Gastropoda) dos Açores. University of the Azores. Unpublished PhD thesis, 329 pp.

Ávila, S.P., Amen, R., Azevedo, J.M.N., Cachão, M., García-Talavera, F., 2002. Checklist of the Pleistocene marine molluscs of Prainha and Lagoinhas (Santa Maria Island, Azores). Açoreana 9 (4), 343–370.

Ávila, S.P., Madeira, P., Mendes, N., Rebelo, A.C., Medeiros, A., Gomes, C., García-Talavera, F., Silva, C.M., Cachão, M., Hillaire-Marcel, C., Martins, A.M.F., 2008. Mass extinctions in the Azores during the last glaciation: fact or myth? J. Biogeogr. 35, 1123–1129.

Ávila, S.P., Madeira, P., Zazo, C., Kroh, A., Kirby, M., da Silva, C.M., Cachão, M., Martins, A.M.F., 2009a. Palaeoecology of the Pleistocene (MIS 5.5) outcrops of Santa Maria Island (Azores) in a complex oceanic tectonic setting. Palaeogeogr. Palaeoclimatol. Palaeoecol. 274 (1–2), 18–31.

Ávila, S.P., Silva, C.M., Schiebel, R., Cecca, F., Backeljau, T., Martins, A.M.F., 2009b. How did they get here? Bulletin de La Société Géologique de France 4 (180), 295–307.

Ávila, S.P., Rebelo, A.C., Medeiros, A., Melo, C., Gomes, C., Bagaço, L., Madeira, P., Borges, P.A., Monteiro, P., Cordeiro, R., Meireles, R., Ramalho, R.S., 2010. Os fósseis de Santa Maria (Açores). 1. A jazida da Prainha, 103 pp.. In: OVGA – Observatório Vulcanológico e Geotérmico dos Açores, Lagoa.

Ávila, S.P., Cordeiro, R., Rodrigues, A.R., Rebelo, A.C., Melo, C., Madeira, P., Pyenson, N. D., 2015a. Fossil Mysticeti from the Pleistocene of Santa Maria Island, Azores (Northeast Atlantic Ocean), and the prevalence of fossil cetaceans on oceanic islands. Palaeontol. Electron. 18.2.27A, 1–12.

Ávila, S.P., Melo, C., Silva, L., Ramalho, R.S., Quartau, R., Hipólito, A., Cordeiro, R., Rebelo, A.C., Madeira, P., Rovere, A., Hearty, P.J., Henriques, D., da Silva, C.M., Martins, A.M.F., Zazo, C., 2015b. A review of the MIS 5e highstand deposits from Santa Maria Island (Azores, NE Atlantic): palaeobiodiversity, palaeoecology and palaeobiogeography. Quat. Sci. Rev. 114, 126–148.

Ávila, S.P., Melo, C., Berning, B., Cordeiro, R., Landau, B., da Silva, C.M., 2016a. *Persististrombus coronatus* (Mollusca: Strombidae) in the lower Pliocene of Santa Maria Island (Azores, NE Atlantic): Paleoecology, paleoclimatology and paleobiogeographic implications. Palaeogeogr. Palaeoclimatol. Palaeoecol. 441, 912–923.

Ávila, S.P., Cachão, M., Ramalho, R.S., Botelho, A.Z., Madeira, P., Rebelo, A.C., Cordeiro, R., Melo, C., Hipólito, A., Ventura, M.A., Lipps, J.H., 2016b. The palaeontological heritage of Santa Maria Island (Azores: NE Atlantic): a re-evaluation of geosites in GeoPark Azores and their use in geotourism. Geoheritage 8, 155–171.

Ávila, S.P., Paris, R., Ramalho, R.S., Rolán, E., González, E.M., Melo, C.S., Cordeiro, R., Madeira, J., 2017. Glacial-age tsunami deposits prove the tropical-ward geographical range expansion of marine cold-water species. In: 5th International Tsunami Field Symposium, Lisbon, 3–7 September.

Ávila, S.P., Ramalho, R., Habermann, J., Titschack, J., 2018a. The marine fossil record at Santa Maria Island (Azores). In: Kueppers, U., Beier, C. (Eds.), Volcanoes of the Azores. Revealing the Geological Secrets of the Central Northern Atlantic Islands. Active Volcanoes of the World, Springer, Berlin, Heidelberg, pp. 155–196.

Ávila, S.P., Cordeiro, R., Madeira, P., Silva, L., Medeiros, A., Rebelo, A.C., Melo, C., Neto, A.I., Haroun, R., Monteiro, A., Rijsdijk, K., Johnson, M.E., 2018b. Global change impacts on large-scale biogeographic patterns of marine organisms on Atlantic oceanic islands. Mar. Pollut. Bull. 126, 101–112. https://doi.org/10.1016/j.marpolbul.2017.10.087.

Ávila, S.P., Melo, C., Sá, N., Quartau, R., Rijsdijk, K., Ramalho, R.S., Berning, B., Cordeiro, R., de Sá, N.C., Pimentel, A., Baptista, L., Medeiros, A., Gil, A., Johnson, M.E., 2019. Towards a "Sea-Level Sensitive Marine Island Biogeography" model: the impact of glacio-eustatic oscillations in global marine island biogeographic patterns. Biol. Rev. 94 (3), 1116–1142.

Ávila, S.P., Azevedo, J.M.N., Madeira, P., Cordeiro, R., Melo, C.S., Baptista, L., Torres, P., Johnson, M.E., Vullo, R., 2020. Pliocene and Late-Pleistocene actinopterygian fishes from Santa Maria Island (Azores: NE Atlantic Ocean): systematics, palaeoecology and palaeobiogeography. Geol. Mag. 157 (9), 1526–1542. https://doi.org/10.1017/S0016756820000035.

Ávila, S.P., Ramalho, R.S., da Silva, C.M., Uchman, A., Berning, B., Johnson, M.E., Melo, C.S., Madeira, P., Rebelo, A.C., Câmara, R., Quartau, R., Baptista, L., Arruda, S., Hipólito, A., González, E., Rasser, M.W., Raposo, V., Pombo, J., Cachão, M., Madeira, J., 2023. Os fósseis de Santa Maria (Açores). 3. O trilho marítimo da Rota dos Fósseis, 120 pp. OVGA – Observatório Vulcanológico e Geotérmico dos Açores. Lagoa. ISBN: 978-989-8164-27-8.

Ávila, S.P., Paris, R., Ramalho, R.S., Melo, C.S., Martín-González, E., Rolán, E., Madeira, P., Ávila, G.C., Porteiro, J.M., Medeiros, A.M., Naughton, F., Abrantes, F., Martins, G.M., Johnson, M.E., Madeira, J., 2025. Mega-tsunami deposits and range expansion of cold-water/temperate marine species towards the tropics in glacial times. Front. Biogeogr. 18, e138319.

Awati, P.R., Rai, H.S., 1931. Ostrea Cucullata: The Bombay Oyster. Methodist Publishing House.

Baarli, B.G., Santos, A.G., Mayoral, E.J., Ledesma-Vázquez, J., Johnson, M.E., Silva, C.M., Cachão, M., 2013. What Darwin did not see: Pleistocene fossil assemblages on a high-energy coast at Ponta das Bicudas, Santiago, Cape Verde Islands. Geological Magazine 150 (1), 183–189.

Baarli, G., Malay, M., Santos, A., Johnson, M., Silva, C.M., Meco, J., Cachão, M., Mayoral, E., 2017. Miocene to Pleistocene transatlantic dispersal of Ceratoconcha coral-dwelling barnacles and North Atlantic island biogeography. Palaeogeogr. Palaeoclimatol. Palaeoecol. 468, 520–528.

Barbera, C., Bordehore, C., Borg, J.A., Glémarec, M., Grall, J., Hall-Spencer, J.M., Huz, Ch., Lanfranco, E., Lastra, M., Moore, P.G., Mora, J., Pita, M.E., Ramos-Esplá, A. A., Rizzo, M., Sánchez-Mata, A., Seva, A., Schembri, P.J., Valle, C., 2003. Conservation and management of northeast Atlantic and Mediterranean maerl beds. Aquat. Conserv. Mar. Freshwat. Ecosyst. 13, S65–S76.

Bassi, D., Iryu, Y., Nebelsick, J.H., 2012. To be or not to be a fossil rhodolith? Analytical methods for studying fossil rhodolith deposits. J. Coast. Res. 28, 288–295.

Basso, D., Brusoni, F., 2004. The molluscan assemblage of a transitional environment: the Mediterranean maerl from off the Elba Island (Tuscan Arcipelago, Tyrrhenian Sea). Bolletino Malacologico 40, 37–45.

Baumann, K.-H., Freitag, T., 2004. Pleistocene fluctuations in the northern Benguela current system as revealed by coccolith assemblages. Mar. Micropaleontol. 52 (1–4), 195–215.

Bebiano, J.B., 1932. A geologia do Arquipélago de Cabo Verde. Comunicações dos Serviços Geológicos de Portugal 18, 1–275.

Billups, K., Vizcaíno, M., Chiarello, J., Kaiser, E.A., 2020. Reconstructing western boundary current wtability in the North Atlantic Ocean for the past 700 kyr from *Globorotalia truncatulinoides* coiling ratios. Paleoceanogr. Paleoclimatol. 35. https://doi.org/10.1029/2020PA003958 e2020PA003958.

Bintanja, R., van de Wal, R.S., Oerlemans, J., 2005. Modelled atmospheric temperatures and global sea levels over the past million years. Nature 437 (7055), 125–128.

Birkett, D.A., Maggs, C.A., Dring, M.J., 1998. Maerl, Volume V: An Overview of Dynamic and Sensitivity Characteristics for Conservation Management of Marine SACs. Marine SACs Project Scottish Association for Marine Science, Scotland. U.K, 116 pp.

Bollmann, J., Baumann, K.-H., Thierstein, H.R., 1998. Global dominance of *Gephyrocapsa* coccoliths in the late Pleistocene: Selective dissolution, evolution, or global environmental change? Paleoceanography 13 (5), 517–529.

Borcard, D., Gillet, F., Legendre, P., 2011. Numerical Ecology with R, 306 pp, 1st ed. Springer-Verlag, New York, U.S.A.

Bosence, D.W.J., 1976. Ecological studies on two unattached coralline algae from Western Ireland. Palaeontology 19 (2), 365–395.

Bosence, D.W.J., 1979. Live and dead faunas from coralline algal gravels, Co. Galway. Palaeontology 22, 449–478.

Budd, A.F., Johnson, K.G., Stemann, T.A., 1996. Plio-Pleistocene turnover and extinctions in the Caribbean reef-coral fauna. In: Jackson, J.B.C., Budd, A.F., Coates, A.G. (Eds.), Evolution and Environment in Tropical America. University of Chicago Press, Chicago, pp. 168–204.

Bulian, F., Jicha, B., Komen, R., Marra, F., Mazzini, I., Scarponi, D., Seijmonsbergen, A. C., Sevink, J., Vannoli, P., Anzidei, M., Monaco, L., Palladino, D.M., Sposato, A., 2025. The MIS 5 marine terraces on the Tyrrhenian Sea coast of Central Italy between Civitavecchia and the Fiora River. Catena 251, 108817.

Cabero, A., 2009. Registro costero de los cambios eustáticos y climáticos durante los interglaciares recientes cuaternarios: Sur y Sureste peninsular, islas Baleares, Canarias y Cabo Verde, 451 pp. Unpublished PhD thesis. Departamento de Geología, Facultad de Ciencias, Universidad de Salamanca.

Cabero, A., González-Delgado, J.Á., Zazo, C., Goy, J.L., Dabrio, C.J., Lario, J., Bardají, T., Hillaire-Marcel, C., Ghaleb, B., 2010. Major migration of the Senegalese warm fauna in the Mediterranean during MIS 5. In: In: Lamolda, M.A., Díaz, E., Moreno, G.J., Maurrasse, F.J.-M.R., Meléndez, G., Paul, C.R.C., Tovar F.J.R. (Eds.), International Conference on Geoevents, Geological Heritage, and the Role of the IGCP, pp. 116–118.

Capet, X., Estrade, P., Machu, E., Ndoye, S., Grelet, J., Lazar, A., Marié, L., Dausse, D., Brehmer, P., 2017. On the dynamics of the southern Senegal upwelling center: observed variability from synoptic to superinertial scales. J. Phys. Oceanogr. 47 (1), 155–180.

Cheng, H., Edwards, R.L., Hoff, J., Gallup, C.D., Richards, D.A., Asmerom, Y., 2000. The half-lives of uranium-234 and thorium-230. Chem. Geol. 169, 17–33.

Clark, P.U., Huybers, P., 2009. Interglacial and future sea level. Geophys. Res. Lett. 462, 856–857.

Clauzel, T., Maréchal, C., Fourel, F., Barral, A., Amiot, R., Betancort, J., Lomoschitz, A., Meco, J., Lécuyer, C., 2020. Reconstruction of sea-surface temperatures in the Canary Islands during Marine Isotope Stage 11. Quat. Res. 94, 195–209.

Cosel, R., 1982. Marine mollusken der Kapverdischen Inseln. Übersicht mit zoogeographischen Ammerkungen. Cour. Forschungsinst. Senck. 52, 35–76.

Cosel, R.C., Gofas, S., 2019. Marine Bivalves of Tropical West Africa, 1102 pp. In: IRD Éditions/MNHN Collection Faune et Flore tropicales n° 48, Muséum national d'Histoire naturelle, Paris Institut de Recherche pour le Développement, Marseille, France.

Costa, F.L., Nunes, M.C., 2008. A precipitação como factor de erosão hídrica na bacia da Ribeira Seca, Santiago, Cabo Verde. In: Workshop Internacional Sobre Clima e Recursos Naturais Nos Países de Língua Portuguesa: Parcerias Na Área Do Clima e Ambiente, pp. 1–11.

Costa, P.J., Dawson, S., Ramalho, R.S., Engel, M., Dourado, F., Bosnic, I., Andrade, C., 2021. A review on onshore tsunami deposits along the Atlantic coasts. Earth Sci. Rev. 212, 103441.

Crocker, A.J., Naafs, B.D.A., Westerhold, T., James, R.H., Cooper, M.J., Röhl, U., Pancost, R.D., Xuan, C., Osborne, C.P., Beerling, D.J., Wilson, P.A., 2022. Astronomically controlled aridity in the Sahara since at least 11 million years ago. Nat. Geosci. 15, 671–676. https://doi.org/10.1038/s41561-022-00990-7.

Dapporto, L., Ramazzotti, M., Fattorini, S., Talavera, G., Vila, R., Dennis, R., 2013. Recluster: an unbiased clustering procedure for beta-diversity turnover. Ecography 36, 1070–1075.

Dapporto, L., Fattorini, S., Voda, R., Dinca, V., Vila, R., 2014. Biogeography of western Mediterranean butterflies: combining turnover and nestedness components of faunal dissimilarity. J. Biogeogr. 41, 1639–1650.

Dapporto, L., Ramazzotti, M., Fattorini, S., Vila, R., Talavera, G., Dennis, R.H.L., 2015. Recluster: ordination methods for the analysis of beta-diversity indices. R package version 2, 8.

Darwin, C., 1839. In: FitzRoy, R. (Ed.), Journal and Remarks, 1832–1836. In Narrative of the Surveying Voyages of his Majesty's Ships Adventure and Beagle between the Years 1826 and 1836, vol. 3. Henry Colburn, London, 615 pp.

Darwin, C., 1844. Geological Observations on the Volcanic Islands Visited during the Voyage of the H.M.S. Beagle. Smith, Elder & Co., London, 175 pp.

Debenay, J.P., Tack, D.L., Ba, M., Sy, I., 1994. Environmental conditions, growth and production of *Anadara senilis* (Linnaeus, 1758) in a Senegal lagoon. J. Molluscan Stud. 60 (2), 113–121.

del Valle, T., 2012. Comparative Growth Rates of the Extinct Coral *Montastraea nancyi*: A Dominant Framework Builder in the Pleistocene (MIS 5e) Reefs of Curaçao, Netherland Antilles. Master Thesis. University of Cincinnati, Department of Geology of the College of Arts and Sciences, 23 pp.

DEM, 2010. Digital Elevation Model of Santiago Island, at 1:5000 scale. Unidade de Coordenação do Cadastro Predial (UCCP) do Ministério do Ambiente, Habitação e Ordenamento do Território (MAHOT). Cabo Verde (2010).

Dittmann, S., 2000. Zonation of benthic communities in a tropical tidal flat of north-East Australia. J. Sea Res. 43, 33–51.

Djangmah, J.S., Shumway, S.E., Davenport, J., 1979. Effects of fluctuating salinity on the behaviour of the West African blood clam *Anadara senilis* and on the osmotic pressure and ionic concentrations of the haemolymph. Mar. Biol. 50, 209–213.

Doney, S.C., Ruckelshaus, M., Duffy, J.E., Barry, J.P., Chan, F., English, C.A., English, C. A., Galindo, H.M., Grebmeier, J.M., Hollowed, A.B., Knowlton, N., Polovina, J., Rabalais, N.N., Sydeman, W.J., Talley, L.D., 2012. Climate Change Impacts on Marine Ecosystems. Annu. Rev. Mar. Sci. 4, 11–37.

Dray, S., Dufour, A.B., 2007. The ade4 package: implementing the duality diagram for ecologists. J. Stat. Softw. 22 (4), 1–20.

Dutton, A., Lambeck, K., 2012. Ice volume and Sea Level during the last Interglacial. Science 337 (6091), 216–219.

Dye, A.H., 1989. Studies on the ecology of *Saccostrea cucullata* (born, 1778) (Mollusca: Bivalvia) on the east coast of southern Africa. J. Zool. 24–2, 110–115.

Flemming, B.W., 2000. A revised textural classification of gravel-free muddy sediments on the basis of ternary diagrams. Cont. Shelf Res. 20 (10–11), 1125–1137.

Folk, R.L., Ward, W.C., 1957. Brazos River Bar: a study in the significance of grain size parameters. J. Sediment. Petrol. 27 (1), 3–26.

Freitas, R., Romeiras, M., Silva, L., Cordeiro, R., Madeira, P., González, J.A., Wirtz, P., Falcón, J.M., Brito, A., Floeter, S.R., Afonso, P., Porteiro, F., Vieira-Rodríguez, M.A., Neto, A.I., Haroun, R., Farminhão, J.N.M., Rebelo, A.C., Baptista, L., Melo, C.S., Martínez, A., Nuñez, J., Berning, B., Johnson, M.E., Ávila, S.P., 2019. Restructuring of the "Macaronesia" biogeographic unit: a marine multi-taxon biogeographical approach. Sci. Rep. 9, 15792.

García-Talavera, F., 1999. Fauna Malacológica del Cuaternario Marino de Cabo Verde. Revista de la Academia Canaria de Ciencias 11 (3–4), 3–25.

García-Talavera, F., Sánchez-Pinto, L., 2001. Moluscos marinos fósiles de Selvagem Pequenha e Ilheu de Fora (Islas Salvajes). Descripción de uma nueva especie de neogasterópodo. Revista de la Academia Canaria de Ciencias 13 (4), 9–21.

Garilli, V., 2011. Mediterranean Quaternary interglacial molluscan assemblages: Palaeobiogeographical and palaeoceanographical responses to climate change. Palaeogeogr. Palaeoclimatol. Palaeoecol. 312 (1–2), 98–114.
Gerber, J., Hemmen, J., Groh, K., 1989. Eine pleistozäne marine Molluskenfauna von Porto Santo (Madeira–Archipel). Mitteilungen der Deutschen Malakozoologischen Gesellschaft 44–45, 19–30.
Govin, A., Capron, E., Tzedakis, P.C., Verheyden, S., Ghabelb, B., Hillaire-Marcel, C., St-Onge, G., Stoner, J.S., Bassinot, F., Bazin, L., Blunier, T., Combourieu-Nebout, N., El Ouahabi, A., Genty, D., Gersonde, R., Jimenez-Amat, P., Landais, A., Martrat, B., Masson-Delmotte, V., Parrenin, F., Seidenkrantz, M.-S., Veres, D., Waelbroeck, C., Zahn, R., 2015. Sequence of events from the onset to the demise of the last Interglacial: evaluating strengths and limitations of chronologies used in climatic archives. Quat. Sci. Rev. 129, 1–36.
Grall, J., Le Loch, F., Guyonnet, B., Riera, P., 2006. Community structure and food web based on stable isotopes (δ15N and δ13C) analyses of a North Eastern Atlantic maerl bed. J. Exp. Mar. Biol. Ecol. 338, 1–15.
Grant, K.M., Amarathunga, U., Amies, J.D., Hu, P., Qian, Y., Penny, T., Rodriguez-Sanz, L., Zhao, X., Heslop, D., Liebrand, D., Hennekam, R., Westerhold, T., Gilmore, S., Lourens, L.J., Roberts, A.P., Rohling, E.J., 2022. Organic carbon burial in Mediterranean sapropels intensified during Green Sahara periods since 3.2 Myr ago. Commun. Earth Environ. 3, 11. https://doi.org/10.1038/s43247-021-00339-9.
Hachich, N.F., Bonsall, M.B., Arraut, E.M., Barneche, D.R., Lewinsohn, T.M., Floeter, S. R., 2015. Island biogeography: patterns of marine shallow-water organisms in the Atlantic Ocean. J. Biogeogr. 42, 1871–1882.
Hachich, N.F., Ferrari, D.S., Quimbayo, J.P., Pinheiro, H.T., Floeter, S.R., 2019. Island biogeography of marine shallow-water organisms. In: Encyclopedia of the World's Biomes. Elsevier, New York. https://doi.org/10.1016/B978-0-12-409548-9.11947-5.
Hansen, J., Sato, M., Hearty, P., Ruedy, R., Kelley, M., Masson-Delmotte, V., Russell, G., Tselioudis, G., Cao, J., Rignot, E., Velicogna, I., Kandiano, E., Schuckmann, K., Kharecha, P., Legrande, A.N., Bauer, M., Lo, K.-W., 2015. Ice melt, sea level rise and superstorms: evidence from paleoclimate data, climate modeling, and modern observations that 2°C global warming is highly dangerous. Atmospheric Chemistry and Physics Discussions 15 (14), 20059–20179.
Haq, B.U., Hardenbol, J., Vail, P.R., 1987. Chronology of Fluctuating Sea Levels since the Triassic. Science 235, 1156–1166.
Harvey, A.S., Bird, F.L., 2008. Community structure of a rhodolith bed from cold-temperate waters (southern Australia). Aust. J. Bot. 56, 437–450.
Hearty, P.J., Tormey, B.R., 2017. Sea-level change and superstorms: geologic evidence from the last interglacial (MIS 5e) in the Bahamas and Bermuda offers ominous prospects for a warming Earth. Mar. Geol. 390, 347–365.
Hearty, P.J., Kindler, P., Cheng, H., Edwards, R.L., 1999. A +20 m middle Pleistocene Sea-level highstand (Bermuda and the Bahamas) due to partial collapse of Antarctic ice. Geology 27, 375–378. https://doi.org/10.1130/0091-7613(1999)0272.3.CO;2.
Helmke, J.P., Bauch, H.A., Röhl, U., Kandiano, E.S., 2008. Uniform climate development between the subtropical and subpolar Northeast Atlantic across marine isotope stage 11. Clim. Past 4 (3), 181–190. https://doi.org/10.5194/cp-4-181-2008.
Hoffman, J.S., Clark, P.U., Parnell, A.C., He, F., 2017. Regional and global sea-surface temperatures during the last interglaciation. Science 355 (6322), 276–279.
Hu, H.-M., Marino, G., Pérez-Mejías, C., Spötl, C., Yokoyama, Y., Yu, J., Rohling, E., Kano, A., Ludwig, P., Pinto, J.G., Michel, V., Valensi, P., Zhang, X., Jiang, X., Mii, H.-S., Chien, W.-Y., Tsai, H.-C., Sung, W.-H., Hsu, C.-H., Starnini, E., Zunino, M., Shen, C.-C., 2024. Sustained North Atlantic warming drove anomalously intense MIS 11c interglacial. Nat. Commun. 15, 5933. https://doi.org/10.1038/s41467-024-50207-1.
Hurley, C., 2012. Gclus: Clustering Graphics. R package version 1 (3), 1.
Hyzny, M., Melo, C.S., Ramalho, R.S., Cordeiro, R., Madeira, P., Baptista, L., Rebelo, A.C., Gómez, C., Torres, P., Uchman, A., Johnson, M.E., Berning, B., Ávila, S.P., 2021. Pliocene and late Pleistocene (MIS 5e) decapod crustacean crabs from Santa Maria Island (Azores Archipelago: NE Atlantic): systematics, palaeoecology and palaeobiogeography. J. Quat. Sci. 36, 91–109. https://doi.org/10.1002/jqs.3261.
Jaccard, P., 1901. Étude comparative de la distribution florale dans une portion des Alpes et des Jura. Bulletin de la Société vaudoise des sciences naturelles 37, 547–579.
Johnson, M.E., Baarli, B.G., Cachão, M., Silva, C.M., Ledesma-Vázquez, J., Mayoral, E.J., Ramalho, R.S., Santos, A., 2012. Rhodoliths, uniformitarianism, and Darwin: Pleistocene and recent carbonate deposits in the Cape Verde and Canary archipelagos. Palaeogeogr. Palaeoclimatol. Palaeoecol. 329–330, 83–100.
Johnson, M.E., Ledesma-Vázquez, J., Ramalho, R.S., Silva, C.M., Rebelo, A.C., Santos, A., Baarli, B.G., Mayoral, E., Cachão, M., 2017. Taphonomic Range and Sedimentary Dynamics of Modern and Fossil Rhodolith Beds: Macaronesian Realm (North Atlantic Ocean). Rhodolith/Maërl Beds: A Global Perspective. https://doi.org/10.1007/978-3-319-29315-8_9.
Johnson, M.E., Silva, C.M., Santos, A., Baarli, B.G., Cachão, M., Mayoral, E., Rebelo, A.C., Ledesma-Vázquez, J., 2011. Rhodolith transport and immobilization on a volcanically active rocky shore: Middle Miocene at Cabeço das Laranjas on Ilhéu de Cima (Madeira Archipelago, Portugal). Palaeogeography, Palaeoclimatology, Palaeoecology 300 (1–4), 113–127.
Jones, C.G., Lawton, J.H., Shachak, M., 1994. Organisms as ecosystem engineers. Oikos 69, 373–386.
Joshi, S., Patrick, G., Brown, C., 2017. Mobility of maerl-siliciclastic mixtures: Impact of waves, currents and storm events. Estuar. Coast. Shelf Sci. 189, 173–188.
Kleinen, T., Hildebrandt, S., Prange, M., Rachmayani, R., Müller, S., Bezrukova, E., Brovkin, V., Tarasov, P.E., 2014. The climate and vegetation of Marine Isotope Stage 11–model results and proxy-based reconstructions at global and regional scale. Quat. Int. 348, 247–265.
Kominz, M.A., Browning, J.V., Miller, K.G., Sugarman, P.J., Mizintseva, S., Scotese, C.R., 2008. Late cretaceous to Miocene Sea-level estimates from the New Jersey and Delaware coastal plain coreholes: an error analysis. Basin Res. 20 (2), 211–226.
Kreft, H., Jetz, W., 2010. A framework for delineating biogeographic regions based on species distributions. J. Biogeogr. 37, 2029–2053.
Kristensen, E., 2008. Mangrove crabs as ecosystem engineers; with emphasis on sediment processes. J. Sea Res. 59, 30–43.
Lavaud, R., Thébault, J., Lorrain, A., van der Geest, M., Chauvaud, L., 2013. *Senilia senilis* (Linnaeus, 1758), a biogenic archive of environmental conditions on the Banc d'Arguin (Mauritania). J. Sea Res. 76, 61–72.
Lea, D.W., Pak, D.K., Spero, H.J., 2000. Climate impact of late quaternary equatorial Pacific Sea surface temperature variations. Science 289 (5485), 1719–1724.
Lecointre, G., Serralheiro, A., 1966. Sur quelques coquilles vivantes et fossiles de l'Archipel du Cap-Vert. J. Conchol. 105 (4), 216–220.
Legendre, P., Legendre, L., 1998. Numerical ecology, 2nd English ed. Elsevier, Amsterdam. 852 pp.
Lisiecki, L.E., Raymo, M.E., 2005. A Pliocene-Pleistocene stack of 57 globally distributed benthic $\delta^{18}O$ records. Paleoceanography 20 (1), PA1003. https://doi.org/10.1029/2004PA001071.
Loutre, M.F., Berger, A., 2003. Marine Isotope Stage 11 as an analogue for the present interglacial. Glob. Planet. Chang. 36 (3), 209–217.
Madeira, J., Mata, J., Mourão, C., Brum da Silveira, A., Martins, S., Ramalho, R., Hoffmann, D., 2010. Volcano-stratigraphic and structural evolution of Brava Island (Cape Verde) based on $^{40}Ar/^{39}Ar$, U/Th and field constraints. J. Volcanol. Geotherm. Res. 196, 219–235.
Madeira, P., Kroh, A., Cordeiro, R., Meireles, R., Ávila, S.P., 2011. The fossil echinoids of Santa Maria Island, Azores (Northern Atlantic Ocean). Acta Geol. Pol. 61, 243–264.
Madeira, J., Ramalho, R., Hoffmann, D.L., Mata, J., Moreira, M., 2020. A geological record of multiple Pleistocene tsunami inundations in an oceanic island: the case of Maio, Cape Verde. Sedimentology 67 (3), 1529–1552.
Maechler, M., Rousseeuw, P., Struyf, A., Hubert, M., Hornik, K., 2018. cluster: Cluster Analysis Basics and Extensions. R package version 2.0.7–1.
Marques, F.O., Hildenbrand, A., Zeyen, H., Cunha, C., Victória, S.S., 2020. The complex vertical motion of intraplate oceanic islands assessed in Santiago Island, Cape Verde. Geochem. Geophys. Geosyst. 21 (3) e2019GC008754.
Martín-González, E., González-Rodríguez, A., Vera-Peláez, J.L., Lozano-Francisco, M.C., Castillo, C., 2016. Asociaciones de moluscos de los depósitos litorales del Pleistoceno Superior de Tenerife (Islas Canarias, España). Vieraea 44, 87–106.
Martín-González, E., Vera-Peláez, J.L., Castillo, C., Lozano-Francisco, M.C., 2018. New fossil gastropod species (Mollusca: Gastropoda) from the upper Miocene of the Canary Islands (Spain). Zootaxa 4422, 191–218.
Martín-González, E., Galindo, I., Mangas, J., Romero, C., Sánchez, N., González-Rodríguez, A., Coello, J.J., Márquez, A., de Vera, A., Vegas, J., Melo, C.S., 2019. Revisión de los depósitos costeros del estadio isotópico marino 5e (MIS 5e) de Fuerteventura (islas Canarias). Vieraea 46, 667–688.
Mata, J., Martins, S., Mattielli, N., Madeira, J., Faria, B., Ramalho, R.S., Silva, P., Moreira, M., 2017. The 2014–15 eruption and the short-term geochemical evolution of the Fogo volcano (Cape Verde): evidence for small-scale mantle heterogeneity. Lithos 288–289, 91–107.
Mayoral, E., Ledesma-Vázquez, J., Baarli, B.G., Santos, A., Ramalho, R., Cachão, M., Silva, C.M., Johnson, M.E., 2013. Ichnology in oceanic islands; case studies from the Cape Verde Archipelago. Palaeogeogr. Palaeoclimatol. Palaeoecol. 381–382, 47–66.
Mayoral, E., Santos, A., Vintaned, J.A.G., Ledesma-Vázquez, J., Baarli, G., Cachão, M., Silva, C.M., Johnson, M., 2018. Upper Pleistocene trace fossils from Ponta das Bicudas, Santiago, Cape Verde islands: systematics, taphonomy and palaeoenvironmental evolution. Palaeogeogr. Palaeoclimatol. Palaeoecol. 498, 83–98.
McManus, J., Oppo, D., Cullen, J., Healey, S., 2003. Marine Isotope Stage 11 (MIS 11): Analog for Holocene and Future climate? In: Droxler, A.W., Poore, R.Z., Burckle, L.H. (Eds.), Earth's Climate and Orbital Eccentricity: The Marine Isotope Stage 11 Question. American Geophysical Union, Washington, D.C., pp. 69–86
Meco, J., 1977. Los *Strombus* Neógenos y Cuaternarios del Atlántico Euroafricano (Taxonomía, Biostratigrafía y Paleoecología). Paleontología de Canarias. Tomo I. Excmo. Cabildo insular de Gran Canaria (Ed.): 142 pp.
Meco, J., 1981. Neogastrópodos fósiles de las Canarias orientales. Anuario de Estudios Atlánticos 27, 601–615.
Meco, J., Petite-Maire, N., Fontugne, M., Shimmield, G., Ramos, A.J., 1997. The quaternary deposits in Lanzarote and Fuerteventura (eastern Canary Islands, Spain): An overview. In: Meco, J., Petite-Maire, N. (Eds.), Climates of the Past. IUGS-UNESCO-Universidad de Las Palmas de Gran Canaria, Las Palmas de Gran Canaria, pp. 123–136.
Meco, J., Guillou, H., Carracedo, J.C., Lomoschitz, A., Ramos, A.J.G., Rodríguez-Yánez, J.J., 2002. The maximum warmings of the Pleistocene world climate recorded in the Canary Islands. Palaeogeogr. Palaeoclimatol. Palaeoecol. 185, 197–210.
Melo, C.S., Martín-González, E., Silva, C.M., Galindo, I., González-Rodríguez, A., Baptista, L., Rebelo, A.C., Madeira, P., Voelker, A.H.L., Johnson, M.E., Arruda, S.A., Ávila, S.P., 2022a. Range expansion of tropical shallow-water marine molluscs in the NE Atlantic during the last interglacial (MIS 5e): Causes, consequences and utility of ecostratigraphic indicators for the Macaronesian archipelagos. Quat. Sci. Rev. 278, 107377.
Melo, C.S., Martín-González, E., Silva, C.M., Galindo, I., González-Rodríguez, A., Baptista, L., Rebelo, A.C., Madeira, P., Voelker, A.H.L., Johnson, M.E., Arruda, S.A., Ávila, S.P., 2022b. Reply to the comment by Meco et al. on "Range expansion of tropical shallow-water marine molluscs in the NE Atlantic during the last interglacial

(MIS 5e): Causes, consequences and utility of ecostratigraphic indicators for the Macaronesian archipelagos". Quat. Sci. Rev. 288, 107535.
Melo, C.S., Silva, C.M., Scarponi, D., Martín-González, E., Rolán, E., Rojas, A., Martinez, S., Silva, L., Johnson, M.E., Rebelo, A.C., Baptista, L., Voelker, A., Ramalho, R.S., Ávila, S.P., 2023. Palaeobiogeography of NE Atlantic archipelagos during the Last Interglacial (MIS 5e): A molluscan approach to the conundrum of Macaronesia as a marine biogeographic unit. Quat. Sci. Rev. 319, 108313.
Milker, Y., Rachmayani, R., Weinkauf, M.F.G., Prange, M., Raitzsch, M., Schulz, M., Kučera, M., 2013. Global and regional sea surface temperature trends during Marine Isotope Stage 11. Clim. Past 9, 2231–2252. https://doi.org/10.5194/cp-9-2231-2013.
Miller, K.G., Kominz, M.A., Browning, J.V., Wright, J.D., Mountain, G.S., Katz, M.E., Sugarman, P.J., Cramer, B.S., Christie-Blick, N., Pekar, S.F., 2005. The Phanerozoic record of global sea-level change. Science 310, 1293–1298.
Miller, K.G., Mountain, G.S., Wright, J.D., Browning, J.V., 2011. A 180-million-year record of sea level and ice volume variations from continental margin and deep-sea isotopic records. Oceanography 24 (2), 40–53.
Mitchell-Thomé, R.C., 1976. Geology of the Middle Atlantic Islands. Beiträge Zur Regionalen Geologie der Erde 12. Borntraeger (Ed.), Berlin.
Monegatti, P., Raffi, S., 2007. Mediterranean-middle Eastern Atlantic façade: molluscan biogeography & ecobiostratigraphy throughout the late Neogene. Açoreana 5, 126–139.
Monegatti, P., Raffi, S., 2010. The Messinian marine molluscs record and the dawn of the eastern Atlantic biogeography. Palaeogeogr. Palaeoclimatol. Palaeoecol. 297 (1), 1–11.
Montesinos, M., 2011. El clima en el Atlántico norafricano durante los interglaciales MIS 5.5 Y MIS 11.3 a partir de los paleoindicadores Harpa rosea Lamarck 1816 y Saccostrea cucullata (Born, 1780) en el archipiélago canario. Unpublished PhD thesis.. Universidade de Las Palmas de Gran Canária, 225 pp.
Montesinos, M., Ramos, A.J.G., Lomoschitz, A., Coca, J., Redondo, A., Betancort, J.F., Meco, J., 2014. Extralimital Senegalese species during Marine Isotope Stages 5.5 and 11 in the Canary Islands (29° N): Sea surface temperature estimates. Palaeogeogr. Palaeoclimatol. Palaeoecol. 410, 153–163.
Muhs, D.R., Meco, J., Simmons, K.R., 2014. Uranium-series ages of corals, sea level history, and palaeozoogeography, Canary Islands, Spain: an exploratory study for two Quaternary interglacial periods. Palaeogeogr. Palaeoclimatol. Palaeoecol. 394, 99–118.
Ochiai, A., 1957. Zoogeographical studies on the soleoid fishes found in Japan and its neigbouring regions. Bull. Jpn. Soc. Sci. Fish. 22, 526–530.
Oksanen, J., Blanchet, F.G., Friendly, M., Kindt, R., Legendre, P., McGlinn, D., Minchin, P.R., O'Hara, R.B., Simpson, G.L., Solymos, P., Stevens, M.H.H., Szoecs, E., Wagner, H., 2017. vegan: Community Ecology Package. R package version 2.4–2.
O'Mara, N.A., Skonieczny, C., McGee, D., Winckler, G., Bory, A.J.M., Bradtmiller, L.I., Malaizé, B., Polissar, P.J., 2022. Pleistocene drivers of Northwest African hydroclimate and vegetation. Nat. Commun. 13, 3552. https://doi.org/10.1038/s41467-022-31120-x.
Paris, R., Giachetti, T., Chevalier, J., Guillou, H., Frank, N., 2011. Tsunami deposits in Santiago Island (Cape Verde archipelago) as possible evidence of a massive flank failure of Fogos volcano. Sediment. Geol. 239, 129–145.
Paris, R., Ramalho, R.S., Madeira, J., Ávila, S.P., May, S.M., Rixhon, G., Engel, M., Brückner, H., Herzog, M., Schukraft, G., Perez-Torrado, F.J., Rodriguez-González, A., Carracedo, J.C., Giachetti, T., 2018. Megatsunami conglomerates and flank collapses of ocean island volcanoes. Mar. Geol. 395, 168–187.
Past Interglacials Working Group of PAGES, 2016. Interglacials of the last 800000 years. Rev. Geophys. 54, 162–219.
Pavão, D.C., Elias, R.B., Silva, L., 2019. Comparison of discrete and continuum community models: Insights from numerical ecology and Bayesian methods applied to Azorean plant communities. Ecol. Model. 402, 93–106.
Portuguese Instituto Hidrográfico, 2019. World Shoreline. https://www.hidrografico.pt/recursos/files/download_gratuito/Linha_costa_internacional.zip last access on 02-06-2019.
Pufahl, P.K., James, N.P., 2006. Monospecific Pliocene oyster buildups, Murray Basin, South Australia: Brackish water end member of the reef spectrum. Palaeogeogr. Palaeoclimatol. Palaeoecol. 233, 11–33.
R Core Team, 2022. R: A Language and Environment for Statistical Computing. R Foundation for Statistical Computing, Vienna, Austria. https://www.R-project.org/.
Raffi, I., Backman, J., Fornaciari, E., Pälike, H., Rio, D., Lourens, L., Hilgen, F., 2006. A review of calcareous nannofossil astrobiochronology encompassing the past 25 million years. Quat. Sci. Rev. 25, 3113–3137.
Railsback, L.B., Gibbard, P.L., Head, M.J., Voarintsoa, N.R.G., Toucanne, S., 2015. An optimized scheme of lettered marine isotope substages for the last 1.0 million years, and the climatostratigraphic nature of isotope stages and substages. Quat. Sci. Rev. 111, 94–106.
Ramalho, R.S., 2011. Building the Cape Verde Islands. Springer-Verlag, Berlin Heidelberg, Berlin, p. 210.
Ramalho, R.S., Helffrich, G., Schmidt, D.N., Vance, D., 2010a. Tracers of uplift and subsidence in the Cape Verde archipelago. J. Geol. Soc. Lond. 167, 519–538.
Ramalho, R.S., Helffrich, G., Cosca, M., Vance, D., Hoffmann, D., Schmidt, D.N., 2010b. Vertical movements of ocean island volcanoes: insights from a stationary plate environment. Mar. Geol. 275 (1–4), 84–95.
Ramalho, R.S., Helffrich, G., Cosca, M., Vance, D., Hoffmann, D., Schmidt, D.N., 2010c. Episodic swell growth inferred from variable uplift of the Cape Verde hotspot islands. Nat. Geosci. 3 (11), 774–777.
Ramalho, R.S., Quartau, R., Trenhaile, A.S., Mitchell, N.C., Woodroffe, C.D., Ávila, S.P., 2013. Coastal evolution on volcanic oceanic islands: a complex interplay between volcanism, erosion, sedimentation, sea-level change and biogenic production. Earth Sci. Rev. 127, 140–170.
Ramalho, R.S., Brum da Silveira, A., Fonseca, P.E., Madeira, J., Cosca, M., Cachão, M., Fonseca, M.M., Prada, S.N., 2015a. The emergence of volcanic oceanic islands on a slow-moving plate: the example of Madeira Island, NE Atlantic. Geochem. Geophys. Geosyst. 16, 522–537.
Ramalho, R.S., Winckler, G., Madeira, J., Helffrich, G.R., Hipólito, A., Quartau, R., Adena, K., Schaefer, J.M., 2015b. Hazard potential of volcanic flank collapses raised by new megatsunami evidence. Sci. Adv. 1 (9), 1–11.
Ramalho, R.S., Helffrich, G., Madeira, J., Cosca, M., Thomas, C., Quartau, R., Hipólito, A., Rovere, A., Hearty, P.J., Ávila, S.P., 2017. The emergence and evolution of Santa Maria Island (Azores) - the conundrum of uplifting islands revisited. Geol. Soc. Am. Bull. 129 (3/4), 372–391.
Raymo, M., Mitrovica, J.X., 2012. Collapse of Polar Ice Sheets during the stage 11 Interglacial. Nature 483, 453–456.
Rebelo, A.C., Rasser, M.W., Kroh, A., Johnson, M.E., Ramalho, R.S., Melo, C., Uchman, A., Berning, B., Silva, L., Zanon, V., Neto, A.I., Cachão, M., Ávila, S.P., 2016. Rocking around a volcanic island shelf: Pliocene rhodolith beds from Malbusca, Santa Maria Island (Azores, NE Atlantic). Facies 62 (3), 1–31.
Rebelo, A.C., Rasser, M.W., Ramalho, R.S., Johnson, M.E., Melo, C.S., Uchman, A., Quartau, R., Berning, B., Neto, A.I., Mendes, A.R., Basso, D., Ávila, S.P., 2021. Pleistocene coralline algal build-ups on a mid-ocean rocky shore – insights into the MIS 5e record of the Azores. Palaeobiogeogr. Palaeoclimatol. Palaeoecol. 579, 110598.
Rebelo, A.C., Martín-González, E., Melo, C.S., Johnson, M.E., González-Rodríguez, A., Galindo, I., Quartau, R., Baptista, L., Ávila, S.P., Rasser, M.W., 2022. Rhodolith beds and their onshore transport in Fuerteventura Island (Canary Archipelago, Spain). Front. Mar. Sci. 9, 917883. https://doi.org/10.3389/fmars.2022.917883.
Rebelo, A.C., Uchman, A., Johnson, M.E., Melo, C.S., Vegas, J., Galindo, I., Mayoral, E.J., Santos, A., González-Rodríguez, A., Afonso-Carrillo, J., Ávila, S.P., Martín-González, E., 2025. Rhodoliths and trace fossils record stabilization of a fan-delta system: an example from the Mio-Pliocene deposits of Gran Canaria (Canary Islands, Spain). J. Palaeogeogr. https://doi.org/10.1016/j.jop.2025.100266 in press.
Ricchi, A., Quartau, R., Ramalho, R.S., Romagnoli, C., Casalbore, D., da Cruz, J.V., Fradique, C., Vinhas, A., 2018. Marine terrace development on reefless volcanic islands: New insights from high-resolution marine geophysical data offshore Santa Maria Island (Azores Archipelago). Mar. Geol. 406, 42–56.
Ricchi, A., Quartau, R., Ramalho, R.S., Romagnoli, C., Casalbore, D., Zhao, Z., 2020. Imprints of volcanic, erosional, depositional, tectonic and mass-wasting processes in the morphology of Santa. Maria insular shelf. Mar. Geol. 424 (656), 106163.
Rodrigues, T., Voelker, A.H.L., Grimalt, J.O., Abrantes, F., Naughton, F., 2011. Iberian margin sea surface temperature during MIS 15 to 9 (580-300 ka): Glacial suborbital variability versus interglacial stability. Paleoceanography 26, PA1204. https://doi.org/10.1029/2010PA001927.
Rohling, E.J., Braun, K., Grant, K., Kucera, M., Roberts, A.P., Siddall, M., Trommer, G., 2010. Comparison between Holocene and Marine Isotope Stage-11 sea-level histories. Earth Planet. Sci. Lett. 291 (1–4), 97–105.
Rousseeuw, P.J., 1987. Silhouettes: a Graphical Aid to the Interpretation and Validation of Cluster Analysis. J. Comput. Appl. Math. 20, 53–65.
Rovere, A., Raymo, M.E., Vacchi, M., Lorscheid, T., Stocchi, P., Gómez-Pujol, L., Harris, D.L., Casella, E., O'Leary, M.J., Hearty, P.J., 2016. The analysis of last Interglacial (MIS 5e) relative sea-level indicators: Reconstructing Sea-level in a warmer world. Earth Sci. Rev. 159, 404–427.
Santos, A., Mayoral, E., Dumont, C.P., Silva, C.M., Ávila, S.P., Baarli, G.B., Cachão, M., Johnson, M.E., Ramalho, R.S., 2015. Role of environmental change in rock-boring echinoid trace fossils. Palaeogeogr. Palaeoclimatol. Palaeoecol. 432, 1–14.
Schratzberger, M., Ingels, J., 2018. Meiofauna matters: the roles of meiofauna in benthic ecosystems. J. Exp. Mar. Biol. Ecol. 502, 12–25.
Serralheiro, A., 1967. Sobre as praias antigas de algumas ilhas de Cabo Verde. García de Orta 15 (1), 123–138.
Serralheiro, A., 1976. A Geologia da Ilha de Santiago (Cabo Verde). Boletim do Museu e Laboratorio Mineralógico e Geológico da Faculdade de Ciências 14, 157–369.
Shackleton, S., Baggenstos, D., Menking, J.A., Dyonisius, M.N., Bereiter, B., Bauska, T.K., Rhodes, R.H., Brook, E.J., Petrenko, V.V., McConnell, J.R., Kellerhals, T., Häberli, M., Schmitt, J., Fischer, H., Severinghaus, J.P., 2020. Global Ocean heat content in the last Interglacial. Nat. Geosci. 13, 77–81.
Simpson, G.G., 1960. Notes on the measurement of faunal resemblance. Am. J. Sci. 258A, 300–311.
Sokal, R.R., Rohlf, F.J., 1962. The comparison of dendrograms by objective methods. Taxon 11, 33–40.
Sørensen, T., 1948. A method of establishing groups of equal amplitude in plant sociology based on similarity of species and its application to analyses of the vegetation on Danish commons. Kongelige Danske Videnskabernes Selskab 5 (4), 1–34.
Spalding, M.D., Fox, H.E., Allen, G.R., Davidson, N., Ferdaña, Z.A., Finlayson, M., Halpern, B.S., Jorge, M.A., Lombana, A., Lourie, S.A., Martin, K.D., Mcmanus, E., Molnar, J., Recchia, C.A., Robertson, J., 2007. Marine Ecoregions of the World: a Bioregionalization of Coastal and Shelf areas. BioScience 57 (7), 573–583.
Spooner, P.T., Chen, T., Robinson, L.F., Coath, C.D., 2016. Rapid uranium-series age screening of carbonates by laser ablation mass spectrometry. Quat. Geochronol. 31, 28–39.
Spratt, R.M., Lisiecki, L.E., 2016. A Late Pleistocene sea level stack. Clim. Past 12, 1079–1092.
Stein, R., Hefter, J., Gruetzner, J., Voelker, A., Naafs, B.D.A., 2009. Variability of surface-water characteristics and Heinrich-like events in the Pleistocene mid-latitude North

Atlantic Ocean: Biomarker and XRD records from IODP Site U1313 (MIS 16–9). Paleoceanography 24, PA2203. https://doi.org/10.1029/2008PA001639.
Steller, D.L., Riosmena-Rodríguez, R., Foster, M.S., Roberts, C.A., 2003. Rhodolith bed diversity in the Gulf of California: the importance of rhodolith structure and consequences of disturbance. Aquat. Conserv. Mar. Freshwat. Ecosyst. 13, S5–S20.
Stirling, C.H., Esat, T.M., Lambeck, K., McCulloch, M.T., 1998. Timing and duration of the last Interglacial: evidence for a restricted interval of widespread coral reef growth. Earth Planet. Sci. Lett. 160 (3–4), 745–762.
Strahler, A.N., 1952. Hypsometric (area-altitude) analysis of erosional topography. GSA Bull. 63 (11), 1117–1142.
Trenhaile, A.S., 1989. Sea level oscillations and the development of rock coasts. Elsevier Oceanography Series 49, 271–295.
Trenhaile, A.S., 2001. Modeling the Quaternary evolution of shore platforms and erosional continental shelves. Earth Surf. Process. Landf. 26, 1103–1128.
Trenhaile, A.S., 2002. Modeling the development of sloping marine terraces on tectonically mobile rock coasts. Mar. Geol. 185, 341–361.
Tzedakis, P.C., Wolff, E.W., Skinner, L.C., Brovkin, V., Hodell, D.A., McManus, J.F., Raynaud, D., 2012. Can we predict the duration of an interglacial? Clim. Past 8 (5), 1473–1485.
Tzedakis, P.C., Hodell, D.A., Nehrbass-Ahles, C., Mitsui, T., Wolff, E.W., 2022. Marine isotope stage 11c: An unusual interglacial. Quat. Sci. Rev. 284, 107493.
Uchman, A., Johnson, M.E., Cristina, A., Melo, C., Cordeiro, R., Ramalho, R.S., Ávila, S. P., 2016. Vertically-oriented trace fossil *Macaronichnus segregatis* from Neogene of Santa Maria Island (Azores; NE Atlantic) records vertical fluctuations of the coastal groundwater mixing zone on a small oceanic island. Geobios 49, 229–241.
Uchman, A., Quintino, V., Rodrigues, A.M., Johnson, M.E., Melo, C.S., Cordeiro, R., Ramalho, R.S., Ávila, S.P., 2017. The trace fossil *Diopatrichnus santamariensis* nov. isp. – a shell armored tube from Pliocene sediments of Santa Maria Island, Azores (NE Atlantic Ocean). Geobios 50, 459–469.
Uchman, A., Torres, P., Johnson, M.E., Berning, B., Ramalho, R.S., Rebelo, A.C., Melo, C. S., Baptista, L., Madeira, P., Cordeiro, R., Ávila, S.P., 2018. Feeding traces of recent ray fish and occurrences of the trace fossil *Piscichnus waitemata* from the Pliocene of Santa Maria Island, Azores (Northeast Atlantic). Palaios 33 (8), 361–375.
Uchman, A., Johnson, M.E., Ramalho, R.S., Quartau, R., Berning, B., Hipólito, A., Melo, C.S., Rebelo, A.C., Cordeiro, R., Ávila, S.P., 2020. Neogene marine sediments and biota encapsulated between lava flows on Santa Maria Island (Azores, north-east Atlantic): an interplay between sedimentary, erosional, and volcanic processes. Sedimentology 67, 3595–3618.
Varela-Lopes, G.E., Carlos, L., Molion, B., 2014. Precipitation patterns in Cape Verde Islands: Santiago Island Case Study. Atmos. Clim. Sci. 4, 854–865.
Voelker, A.H.L., Rodrigues, T., Billups, K., Oppo, D., McManus, J., Stein, R., Hefter, J., Grimalt, J.O., 2010. Variations in mid-latitude North Atlantic surface water properties during the mid-Brunhes (MIS 9-14) and their implications for the thermohaline circulation. Clim. Past 6, 531–552. https://doi.org/10.5194/cp-6-531-2010.
Wentworth, C.K., 1922. A scale of grade and class terms for clastic sediments. J. Geol. 30 (5), 377–392.
Wilson, S., Blake, C., Berges, J.A., Maggs, C.A., 2004. Environmental tolerances of free-living coralline algae (maerl): implications for European marine conservation. Biol. Conserv. 120, 279–289.
Wolff, W.J., Gueye, A., Meijboom, A., Piersma, T., Sall, M.A., 1987. Distribution, biomass, recruitment and productivity of Anadara senilis (L.) (Mollusca: Bivalvia) on the Banc d'Arguin, Mauritania. Neth. J. Sea Res. 21 (3), 243–253.
WoRMS Editorial Board, 2023. World Register of Marine Species. Available from. https://www.marinespecies.orgatVLIZ.
Yokoyama, Y., Esat, T.M., Thompson, W.G., Thomas, A.L., Webster, J.M., Miyairi, Y., Sawada, C., Aze, T., Matsuzaki, H., Okuno, J., Fallon, S., Braga, J., Humblet, M., Iryu, Y., Potts, D.C., Fujita, K., Suzuki, A., Kan, H., 2018. Rapid glaciation and a two-step sea level plunge into the Last Glacial Maximum. Nature 559, 603–607.
Zazo, C., Goy, J.L., Hillaire-Marcel, C., Gillot, P.-Y., Soler, V., González-Delgado, J.Á., Dabrio, C.J., Ghaleb, B., 2002. Raised marine sequences of Lanzarote and Fuerteventura revisited — a reappraisal of relative sea-level changes and vertical movements in the eastern Canary Islands during the Quaternary. Quat. Sci. Rev. 21 (2002), 2019–2046.
Zazo, C., Goy, J.L., Dabrio, C.J., Bardají, T., Hillaire-Marcel, C., Ghaleb, B., González-Delgada, J.A., Soler, V., 2003a. Pleistocene raised marine terraces of the Spanish Mediterranean and Atlantic Coasts: Records of coastal uplift, sea-level highstands and climate changes. Mar. Geol. 194 (1–2), 103–133.
Zazo, C., Goy, J.L., Hillaire-Marcel, C., Delgado, J.A.G., Soler, V., Ghaleb, B., Dabrio, C.J., 2003b. Registro de los cambios del nivel del mar durante el Cuaternario en las islas Canarias Occidentales (Tenerife y La Palma). Estud. Geol. 59, 133–144.
Zazo, C., Goy, J.L., Dabrio, C.J., Soler, V., Hillaire-marcel, C., Ghaleb, B., 2007. Quaternary marine terraces on Sal Island (Cape Verde archipelago). Quat. Sci. Rev. 26, 876–893.
Zazo, C., Goy, J.L., Hillaire-Marcel, C., Dabrio, C.J., González-Delgada, J.A., Cabero, A., Bardají, T., Ghaleb, B., Soler, V., 2010. Sea level changes during the last and present interglacials in Sal Island (Cape Verde archipelago). Glob. Planet. Chang. 72, 302–317.